Economic Geology
Vol. 68, 1973, pp. 518–539

The Chemical Compositions of Synthetic and Natural Pentlandite Assemblages

KULA C. MISRA AND M. E. FLEET

Abstract

The phase relations of pentlandite assemblages in the Fe-Ni-S system have been reinvestigated by sealed, silica tube annealing experiments at 600°, 500°, 400°, 300°, and 230°C. The compositions of the coexisting phases in the quenched products have been determined by electron probe analyses, so that the phase boundaries are located with much greater accuracy than in previous work and actual tie lines plotted. The tie lines between pentlandite solid solution (pns) and monosulfide solid solution (mss) change direction at a mss composition of about 33 at. % Ni, correlating with the composition at which the mss field breaks down below 400°C. The mss field, continuous at 400°C, extends only to about 25 at. % Ni at 300°C; the other more S-rich phases coexisting with pns at this temperature being a second mss phase, containing about 33 at. % Ni, and β(Ni,Fe)S containing about 5 at. % Fe. The mss field withdraws to 17 at. % Ni at 230°C, enabling pyrite-pns tie lines to be established. At 230°C, the limits of solid solution of Ni in pentlandite are 15 at. % when coexisting with troilite and 34 at. % when coexisting with β(Ni,Fe)S.

Electron probe analyses have been made on a variety of natural pentlandite assemblages. A compilation of data from all sources confirms that the composition of pentlandite varies systematically with the assemblage, ranging from 18 at. % Ni in the assemblage troilite-pentlandite to 34 at. % Ni in the assemblage millerite-heazlewoodite-pentlandite. The Ni content of pyrrhotite and the Fe contents of millerite and heazlewoodite are significantly lower than the corresponding data for the synthetic system at 230°C, suggesting that chemical readjustment persisted to very low temperatures in these assemblages. The good agreement among several limiting compositions in comparing the synthetic and natural data indicates that the principal factors controlling the phase chemistry of natural nickel sulfide assemblages are related to crystal-crystal equilibria.

Introduction

PENTLANDITE is common to almost all natural nickel sulfide assemblages and it is the most important ore mineral of the Ni in these assemblages. The phase of synthetic, and to a lesser extent, natural pentlandite assemblages form extensive solid solutions within the Fe-Ni-S ternary system and the present study arose through a realization of the unique advantages of the electron microprobe analyzer for providing much needed compositional information on them. The study is conveniently divided into three parts: (1) An experimental investigation of parts of the synthetic system, essentially involving a reinvestigation at moderate temperatures, using the electron probe to determine the composition of the coexisting phases, and an extension of these studies to low temperatures; (2) The determination of the compositions of selected natural, and principally, Canadian pentlandite assemblages and the correlation and analysis of compositional data from all sources; (3) The presentation of an interpretative, low temperature phase diagram for natural assemblages, largely developed from a synthesis of the experimental data and the occurrence and compositions of the natural phases.

Experimental Investigations of Parts of the Fe-Ni-S System

Previous work

Phase relations in parts of the Fe-Ni-S system reported by earlier workers (Newhouse, 1927; Vogel and Tonn, 1930; Zurbrigg, 1933; Urazov and Filin, 1938; Colgrove, 1940) are not reliable because their experiments had no provision to prevent the escape of S during annealing. Colgrove (1942), using pressure bombs and sealed glass tubes, and later, Lundqvist (1947a) who investigated the entire system through rigid silica tube, quench-type, annealing experiments, both reported a fairly extensive solid solution field for pentlandite (Table 3). The system was reinvestigated by systematic studies undertaken in the Geophysical Laboratory of the Carnegie Institution, Washington, during the last two decades, mostly through rigid silica tube, quench-type, annealing experiments (Kullerud, 1956, 1962,

1963a, 1963b; Kullerud et al., 1969; Clark and Kullerud, 1963; Naldrett and Kullerud, 1966; Naldrett et al., 1967; Craig, 1967, 1971; Craig and Naldrett, 1971; Craig et al., 1967), and much of our present understanding of the system stems from these studies. Shewman and Clark (1970) examined the monosulfide solid solution (mss)-pentlandite equilibria and outlined the limits of solid solution of pentlandite at various temperatures.

A survey of the literature on the Fe-Ni-S system indicates that the compositions of the phases in these investigations were not determined directly but had been estimated either from the bulk compositions of the charges or from the variations in the lattice parameters, and it was considered that the solid solution fields of the phases could be delineated much more accurately with electron probe analysis of the experimental products. Furthermore the data for natural assemblages suggest final equilibration temperatures significantly lower than the lowest temperature at which the phase relations had been investigated in the laboratory, kinetic factors being prohibitive in experi-

TABLE 1. Details of Annealing Experiments

Charge No.	Annealing Temp. (°C)	Annealing Time (Days)	Bulk Composition (at. %) Fe	Ni	S	Coexisting Phases Identified in Quenched Product
KA-22	700	20	43.19	14.86	41.95	pns, mss, tn
KA-23	700	20	21.11	35.95	41.94	pns, hs, tn
KA-24	700	20	14.15	43.91	41.94	pns, hs, tn
KB-25	600	49	43.19	14.86	41.95	pns, mss, tn
KB-26	600	49	22.11	35.95	41.94	pns, hs, tn
KB-27	600	49	13.82	44.24	41.94	pns, hs, tn
KB-97	598	18	33.93	17.17	48.90	pns, mss
KB-98	598	18	19.67	31.61	48.72	pns, mss
KB-99	598	18	15.04	36.29	48.67	pns, mss, gs
KB-101	596	20	27.74	24.26	48.00	pns, mss
KB-102	596	20	11.82	40.16	48.02	pns, mss, gs
KC-28	500	49	43.19	14.86	41.95	pns, mss, tn
KC-29	500	49	22.11	35.95	41.94	pns, hs, tn
KC-30	500	49	13.82	44.24	41.94	pns, hs, tn
KC-10	500	28	40.97	10.52	48.51	pns, mss
KC-11	500	28	36.29	15.19	48.52	pns, mss
KC-13	500	28	25.75	25.71	48.54	pns, mss
KC-12	500	28	20.37	31.08	48.55	pns, mss
KC-14	500	28	15.57	35.86	48.57	pns, mss
KC-15	500	28	9.58	41.85	48.57	pns, mss, gs
KD-31	399	192	37.31	20.74	41.95	pns, mss, tn
KD-32	399	192	22.11	35.95	41.94	pns, hs, tn
KD-33	399	192	13.82	44.24	41.94	pns, hs, tn
KD-16	400	20	41.93	9.56	48.51	pns, mss, tn
KD-17	400	20	36.29	15.19	48.52	pns, mss
KD-18	400	20	25.76	25.70	48.54	pns, mss
KD-19	398	22	20.36	31.09	48.55	pns, mss
KD-20	398	22	14.72	36.72	48.56	pns, mss
KD-21	398	22	9.58	41.85	48.57	pns, mss, gs
KE-34	300	192	37.31	20.74	41.95	pns, tn
KE-35	300	192	22.11	35.95	41.94	pns, hs, tn
KE-36	300	192	13.82	44.24	41.94	pns, hs, tn
KE-37	300	175	40.91	10.62	48.47	pns, mss(1)
KE-40	300	175	25.76	25.78	48.46	pns, mss(1)
KE-39	300	175	20.76	30.79	48.45	pns, mss(1), mss(2)
KE-41	300	175	15.61	35.94	48.45	pns, mss(2), mls
KE-42	300	175	10.15	41.41	48.44	pns, mls
KF-49	285	202	44.22	13.83	41.95	pns, mss(1), tn
KF-50	285	202	13.82	44.24	41.94	pns, hs, tn
KG-83	230	203	39.83	11.20	48.97	pns, mss(1)
KG-84	230	203	35.41	15.67	48.92	pns, mss(1)
KG-85	230	203	25.45	25.75	48.80	pns, mss(1)
KG-86	230	203	20.82	30.44	48.74	pns, mss(2), mls
KG-87	230	203	15.49	35.84	48.67	pns, mss(2), mls
KG-88	230	203	9.25	42.15	48.60	pns, mls
KG-89	230	203	12.44	45.63	41.93	pns, hs, tn
KG-90	230	203	41.92	16.13	41.95	pns, mss, tn

ments below 300°C. It was decided to extend the present studies to low temperatures using a modified experimental approach to that adopted by previous workers, in an attempt to increase the reaction rates and the reactivity of the reactants.

Experimental

The phase relations in parts of the condensed Fe-Ni-S system were reinvestigated by rigid silica tube, quench-type, annealing experiments at 600°, 500°, 400°, 300°, and 230°C. The starting materials were Koch-Light Laboratories Fe sponge (5N purity) and Ni sponge (5N purity), and Johnson-Matthey "specpure" S crystals. The Fe and Ni sponge were reduced with hydrogen to remove oxygen contamination. The charges (200 mg each) were prepared from stock compositions of binary mixtures of Fe and Ni with S, which had been annealed in vacuum-sealed silica tubes at 700°C for one or two weeks. The bulk compositions of the charges used

TABLE 2. Composition of Coexisting Synthetic Phases in the Fe-Ni-S System (Electron Probe Analyses)

	Compositions of Coexisting Phases, atomic %														
Charge No.	pns			mss			tn			hs			gs		
	Fe	Ni	S	Fe	Ni	S	Fe	Ni	S	Fe	Ni	S	Fe	Ni	S
KB-25	33.29	20.31	46.40	46.00	3.77	50.23	36.14	63.80	0.06						
KB-26	25.46	27.42	47.12				28.19	71.63	0.18						
KB-27	25.81	27.50	46.69							11.26	47.54	41.20			
KB-97	28.04	25.48	46.48	39.56	9.85	50.59									
KB-98	19.91	33.66	46.43	21.56	27.54	50.90									
KB-99	13.57	40.00	46.43	17.00	32.55	50.45							8.20	46.08	45.72
KB-101	25.48	28.23	46.29	34.94	14.36	50.70									
KB-102	11.36	42.58	46.06	14.46	35.34	50.20							8.27	46.27	45.46
KC-28	35.44	17.88	46.68	48.01	2.15	49.84	36.74	62.96	0.30						
KC-29	25.68	27.41	46.91				27.90	71.82	0.28						
KC-30	25.54	27.83	46.63							8.88	49.99	41.13			
KC-10	32.28	20.54	47.18	45.52	4.00	50.48									
KC-11	28.50	24.12	47.38	40.05	9.11	50.84									
KC-13	22.20	31.03	46.77	29.55	19.39	51.06									
KC-12	20.46	32.81	46.73	19.99	29.19	50.82									
KC-14	17.82	35.78	46.40	13.63	36.70	49.67									
KC-15	15.16	38.01	46.83	7.65	42.24	50.11							3.15	50.67	46.18
KD-31	36.38	17.17	46.45	48.01	2.24	49.75									
KD-32	27.09	26.73	46.18				26.68	73.13	0.19	3.65	57.73	38.62			
KD-33	27.09	26.97	45.94							2.70	59.29	38.01			
KD-16	36.84	17.19	45.97	49.08	1.62	49.30	36.27	61.28	2.45						
KD-17	31.44	22.06	46.50	43.94	5.79	50.27									
KD-18	23.45	29.98	46.57	30.95	17.91	51.14									
KD-19	21.17	31.97	46.86	21.82	26.82	51.36									
KD-20	18.47	34.25	47.28	12.85	37.42	49.73									
KD-21	14.03	39.31	46.66	6.15	43.35	50.50							5.46	47.64	46.90
KE-34	37.60	16.03	46.37				47.02	52.76	0.22						
KE-35	27.49	26.15	46.36				27.56	71.96	0.48	2.61	58.07	39.32			
KE-36	25.76	28.08	46.16							3.15	57.28	39.57			
		pns			mss (1)			mss (2)						mls	
KE-37	34.85	18.67	46.48	46.84	3.56	49.60									
KE-40	23.05	30.30	46.65	32.48	16.16	51.36									
KE-39	20.06	33.23	46.71	23.25	24.83	51.92	16.81	32.60	50.59						
KE-41	19.67	33.80	46.53				14.76	34.16	51.08				5.02	46.26	48.72
KE-42	18.45	35.08	46.47										2.44	48.36	49.20
		pns			mss (1)						hs			tn	
KF-49	39.78	14.62	45.60	49.03	1.47	49.50							72.94	26.74	0.32
KF-50	26.61	27.16	46.23							4.40	57.03	38.57			
		pns			mss (1)			mss (2)			hs			mls	
KG-83	32.52	20.68	46.80	45.40	4.72	49.88									
KG-84	27.41	26.39	46.20	41.83	7.05	51.12									
KG-85	23.43	29.64	46.93	31.55	16.68	51.77									
KG-86	20.41	32.19	47.40				18.95	30.05	51.00						
KG-87	20.42	32.32	47.26				20.18	30.11	49.71				5.55	45.52	48.93
KG-88	18.58	34.13	47.29										3.49	47.13	49.38
KG-89	24.45	30.39	45.16							8.42	50.71	40.87			
KG-90	38.76	15.05	46.19	48.70	1.53	49.77									

in these experiments fall on four sections of almost constant S—about 42.0, 48.0, 48.5, and 49.0 at. % S (Table 1). The abbreviations used for the synthetic phases in Tables 1, 2, 4, and in the text are as follows: mss = monosulfide solid solution, $(Fe,Ni)_{1-x}S$; pns = pentlandite solid solution; gs = godlevskite solid solution, α and β $(Ni,Fe)_7S_6$; hs = heazlewoodite solid solution, $(Ni,Fe)_3S_2$; mls = millerite solid solution, $\beta(Ni,Fe)S$; and tn = taenite, face-centered cubic (Fe,Ni) alloy.

Each charge was fused in an oxygen-natural gas flame and quenched in cold water, prior to annealing at a specific temperature in a horizontal tube furnace. Frequent monitoring of the temperature of the charges and estimates of the accuracy of the temperature recording suggests that the recorded temperatures are accurate to ± 3°C. The annealing time varied with temperature, from about three weeks at 600°C to more than six months at 230°C (Table 1). The annealed charges were quenched in cold water and the quenched products were studied with reflected-light microscopy, X-ray powder diffraction techniques, and electron probe analysis.

Fe, Ni, S in each quenched phase were analyzed simultaneously using a three-channel MAC (model 400) electron microprobe analyzer. Two quenched synthetic sulfide preparations, $Fe_{49.87}S_{50.13}$(M-2) and $Ni_{50.00}S_{50.00}$(M-3), were used as standards; the

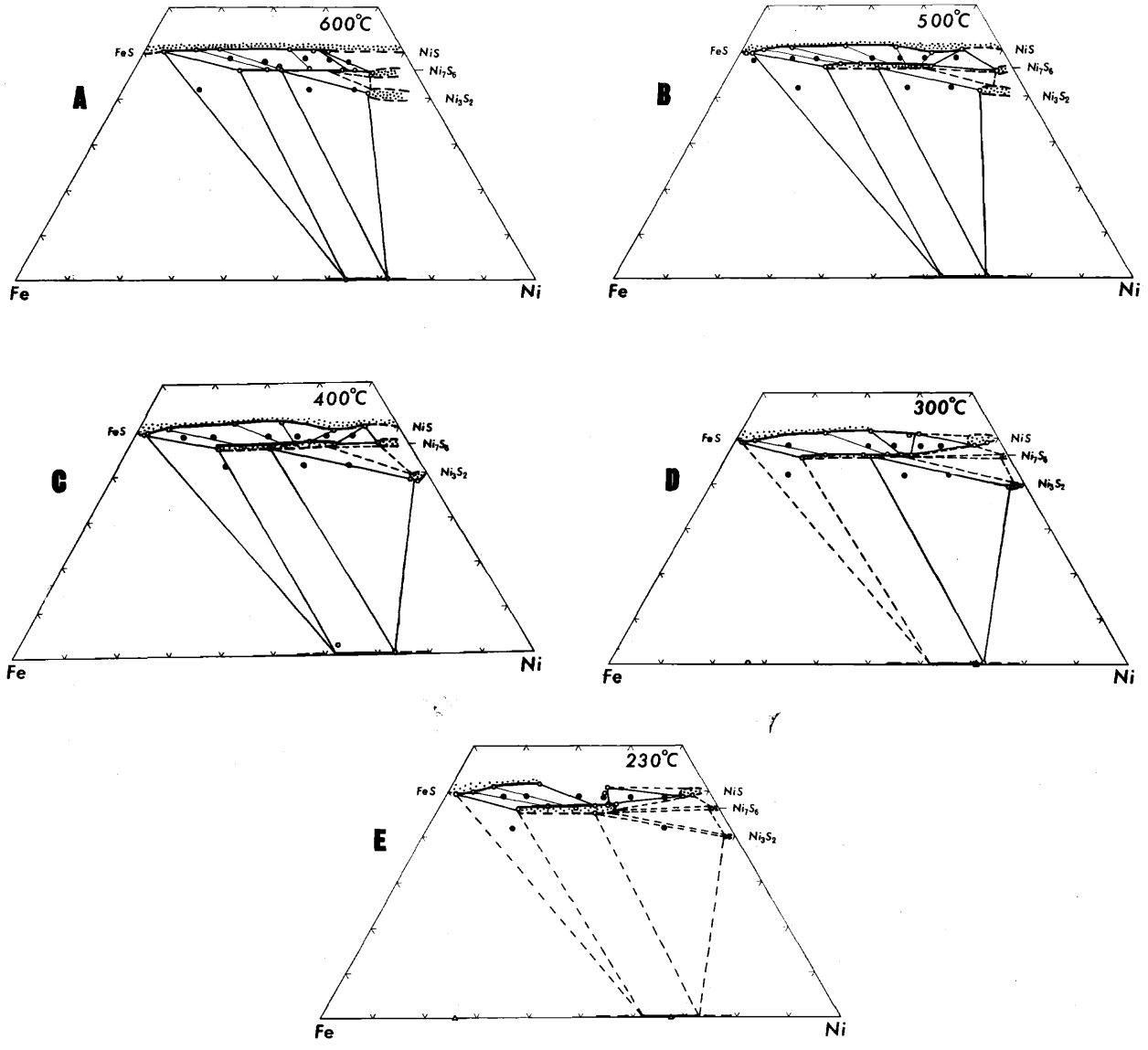

FIG. 1. Phase relations in parts of the condensed Fe-Ni-S system at A) 600°C, B) 500°C, C) 400°C D) 300°C and E) 230°C. Solid circles = bulk compositions; open circles = phase compositions; open triangles = compositions determined by X-ray diffraction; data plotted as atomic percent.

TABLE 3. Solid Solution Limits of Pentlandite

Annealing temp. (°C)	Fe and Ni Solubility Limits: Fe Limit at. % Fe	Fe and Ni Solubility Limits: Ni Limit at. % Ni	S Solubility Limits at Atomic Fe:Ni = 1:1 at. % S	Source of Data
600	33.3	41.3	46.4	This study
500	35.5	38.0	46.2–47.3	
400	36.8	39.3	46.0–46.9	
300	39.8	33.8	46.2–46.6	
230	38.8	34.0	45.2–46.9	
*	30.70	39.8	43.6–47.1	Colgrove (1942)
680, 400, 200	30.71	30.71	47.06	Lundqvist (1947a)
500	33.9	33.3	46.8–47.6	Kullerud (1956)
*	40.00	37.64	47.06	Knop & Ibrahim (1961)
600	27.1	27.7	46.8–47.4	Kullerud (1963b)
500	29.1	29.1	46.2–47.8	
400	27.8	27.7	46.5–47.5	
*	32.94	25.15	46.65–46.78	Popova et al. (1964)
400	31.1	35.1	47.0	Craig et al. (1967)
600	28.75 ± 0.48	31.91 ± 0.55	46.23 ± 0.23–47.92 ± 0.33	Shewman & Clark (1970)
500	33.94 ± 0.31	37.77 ± 1.11	46.70 ± 0.22–47.86 ± 0.27	
400	35.46 ± 0.24	32.07 ± 1.42	46.70 ± 0.22–47.37 ± 0.23	
300	34.82	27.90	46.80–47.14	
200	34.82	27.90	46.80–46.92	

* Cooled to room temperature.

former, consisting of a homogenous pyrrhotite phase, for Fe and S, and the latter, consisting of a mixture of α and β NiS phases, for Ni (Misra, 1972). The operating conditions of the electron probe were as follows: 15 Kv, 0.1μ amp on M-2 standard, counting time 20 secs, and spot diameter of about 3μ. All count data were obtained for Kα lines using LiF (for Fe and Ni) and PET (for S) analyzing crystals. The data were reduced using program EMPADR-IV (Rucklidge, 1967). The precision and accuracy of the analytical results in the present investigation (Table 2) have been estimated to be ± 0.4 at. % for Fe, Ni and S (Misra, 1972). The tn phase in charges KB-27, KC-30, KD-31, KD-33, KE-36, KF-30, KG-89, and KG-90, and the hs phase in KB-26 and KC-29 could not be analyzed because of extremely small grains.

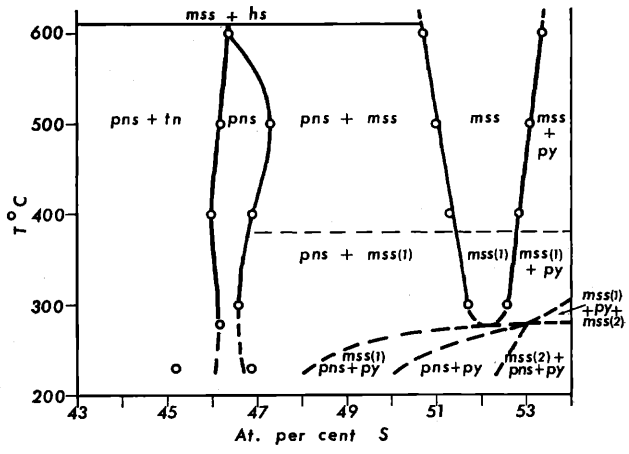

FIG. 2. Section across pns field at Fe:Ni = 1:1. Pentlandite upper stability limit from Kullerud (1963a); mss field S-rich limit from Naldrett, Craig, and Kullerud (1967).

Discussion of the phase relations

The phase relations obstained at the different temperatures of annealing are shown in the respective isothermal sections (Fig. 1). All assemblages shown in these phase diagrams coexist with a vapor phase (v), the vapor pressure for any assemblage varying with temperature and, for any isothermal section, with the compositions and relative proportions of the phases in an assemblage.

Pentlandite solid solution: The Fe and Ni solubility limits of the pns field at a particular temperature have been defined by pns compositions in the univariant assemblages pns-mss-tn-v, and pns-mss-mls-v or pns-mss-gs-v, respectively. The upper S solubility limits at varying Fe:Ni ratios have been determined from the compositions of pns coexisting with mss. However, data for the lower S solubility limit of the pns field at all temperatures of investigation are limited to the univariant assemblage pns-tn-hs-v (with the exception of KE-34 which gave the divariant assemblage pns-tn-v). Without experimental data for compositions of pns coexisting with tn, hs-gs, and gs-mls, the lower S solubility limits of the field, as shown in the isothermal sections, are largely interpretive.

The variations in the solid solution limits of pentlandite with temperature are asymmetrical and somewhat unsystematic (Table 3, Figs. 2 and 3). At 600°C the field extends from 33.3 at. % Fe to a maximum of about 41.3 at. % Ni. The distribution of the pns field is shown only schematically above

this temperature in Figure 3. Previous workers (Naldrett et al., 1967) have indicated a univariant field of FeS-pns-hs-v and a divariant field of FeS-hs-v at 600°C. This differs slightly from our data (below) but would involve a decrease in the breakdown temperature of pns with increasing Fe content and, while disagreeing on the exact rate of this decrease, we have used this report as tentative evidence that the upper stability limit of the pns field is marked by a shallow, domed "surface." The Fe solubility progressively increases with decrease in temperature below 600°C and reaches a maximum of 39.8 at. % Fe at 285°C. The decrease of this limit to 38.8 at. % Fe at 230°C suggests that the solubility of Fe in pns coexisting with mss and tn tends to decrease slightly at lower temperatures. The Ni solubility limit reaches a minimum of 33.8 at. % Ni at 300°C and shows a slight increase at 230°C.

The variations in the M : S ratios of pentlandites are quite small compared to variations in the Fe : Ni ratios. Most of the compositions within the field are less than that for stoichiometric M_9S_8 (47.06 at. % S). The pns has an almost constant S content at 600°C (46.4 at. %), and the field expands asymmetrically on either side of this value at lower temperatures. The upper S solubility limit reaches a maximum of 47.4 at. % S in the Fe-rich portion of the field at 500°C, and maxima of 47.4 at. % S at 230°C and 47.2 at. % S at 400°C in the Ni-rich portion of the field. The field is very narrow at 300°C, with a range of S content between 46.2 and 46.7 at. %. The present data suggest a divergence of the field, principally toward low S compositions, at 230°C. However, the lower S limit of the pns field at this temperature is inferred from one point only for which there is evidence (discussed later) of disequilibrium in the final assemblage.

The Fe and Ni solubility limits determined in the present study are significantly higher than those reported by earlier workers or estimated from their published phase diagrams (Table 3). The saturation limits of the pentlandite field were determined by Knop and Ibrahim (1961) and Shewman and Clark (1970) from discontinuities in the lattice parameter, composition curves, assuming the compositions of the pentlandite phases to be represented by the respective bulk compositions of the annealed charges. This assumption was not generally valid. Further, the lattice parameter, composition curves are insensitive to Ni variations near the high Ni limits and therefore do not allow accurate determination of the Ni saturation limits (Misra, 1972).

Pentlandite was identified in the quenched products of a set of charges KA-22, 23, and 24 (Table 1) annealed at 700°C. Pentlandite is known to be unstable at 700°C but the principal phase in the stable

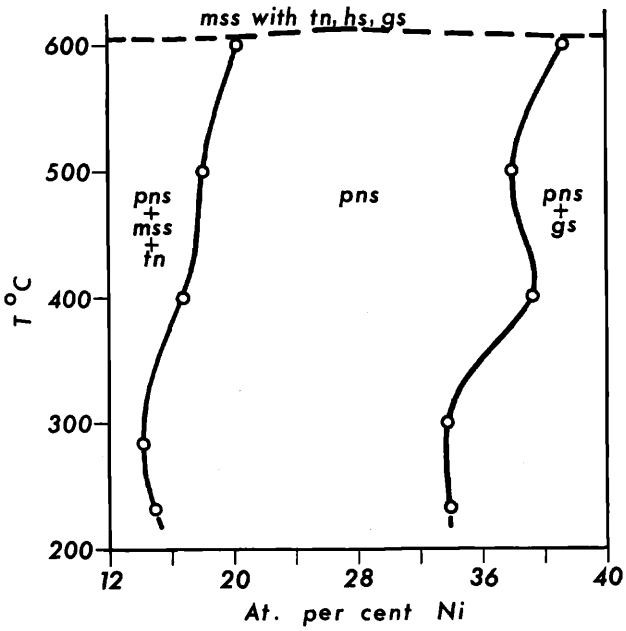

FIG. 3. Section across pns field at 46.4 at. % S.

assemblage for these bulk compositions, $(Ni, Fe)_{3\pm x}S_2$, is unquenchable and readily inverts to pns and hs on quenching below 610°C (Kullerud, 1963a). As expected the pns and hs in these charges were inhomogeneous (Fig. 4), the quenching period being insufficient to allow for the establishment of equilibrium between them.

Monosulfide solid solution: Only the S-poor limits of the mss field were determined in the present study. This boundary (solvus) recedes progressively toward S-rich compositions with falling temperature; its S limits at a section with atomic Fe : Ni ratio 1 : 1 are estimated as 50.7, 51.0, 51.3, and 51.8 at. % S at 600°, 500°, 400°, and 300°C, respectively (Fig. 3). The boundary does not extent to this section at 230°C. Except for the Fe-rich end, the shape and position of the boundary at the temperatures investigated compare well with the data of Naldrett et al. (1967). From the data of the present investigation for the S-poor limits and the data of Naldrett et al. (1967) for the S-rich limits, the S solubility limits of the mss field are found to decrease in a systematic manner from 50.7–53.3 at. % S at 600°C to 51.8–52.7 at. % at 300°C along the section atomic Fe : Ni = 1 : 1 (Fig. 2).

Because of the direct determination of the phase compositions by electron probe analyses, it has been possible to draw real tie lines between coexisting mss and pns phases at different bulk compositions and temperatures, as shown in the phase diagrams. With the exception of the 600°C data, the tie lines change from a negative to a positive slope around a mss composition of about 33 at. % Ni.

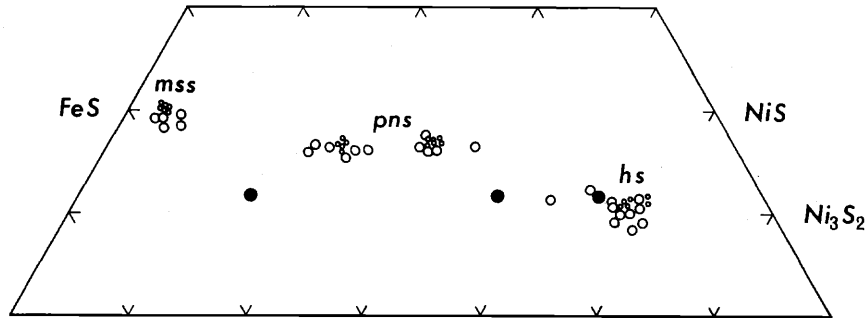

FIG. 4. The grain-to-grain variation in the compositions of mss, pns, and hs in charges quenched from 700°C (large, open circles) compared to similar data for 600°C (small, open circles). Solid circles = bulk compositions.

The mss field, which is continuous between $Fe_{1-x}S$ and $Ni_{1-x}S$ at higher temperatures, breaks down at some temperature between 400° and 300°C, and at a composition of about 33 at. % Ni. The composition is correlatable with the composition at which the tie lines with pns change slope and at which the d_{102} and c-parameter distributions of the mss show a discontinuity (Shewman and Clark, 1970; Misra, 1972). At 300°C the mss field is seen to withdraw away from the Ni-S join and separate into two mss phases, mss(1) and mss(2), with about 25 and 33 at. % Ni, respectively, coexisting with pns (about 33.5 at. % Ni) and vapor as a univariant assemblage (Fig. 1D). The mss(2) phase also forms a part of the univariant field with pns of above composition and β(Ni,Fe)S containing about 5.5 at. % Fe, and is probably related to the more S-rich part of the β(Ni,Fe)S field through a divariant field (mss(2)-mls-v). Thus at 300°C, instead of a continuous solid solution between $Fe_{1-x}S$ and $Ni_{1-x}S$, we get two mss phases, mss(1) and mss(2) through unmixing, and a β(Ni,Fe)S phase through either reaction or unmixing. The breakdown of the mss field occurs at a temperature higher than that reported by previous workers (275 ± 10°C, Shewman and Clark, 1970; 275 ± 25°C, Craig and Naldrett, 1971) though there is very good agreement on the composition of the mss at which this breakdown occurs. At lower temperatures the mss(1) phase withdraws further toward the Fe-S join, to about 17 at. % Ni at 230°C, whereas the mss(2) phase does not show much change from its composition at 300°C. The stabilization of mss(2) at this specific composition (atomic Fe : Ni ratio about 1 : 2) is due perhaps to the stability of a particular ordered arrangement of the metal atoms.

At 230°C, the limiting composition of mss(1) is about 17 at. % Ni, so that the solvus has withdrawn sufficiently to allow tie lines between pyrite and Ni-rich pentlandites to be established. Phase relations in this region have not been investigated in the present study, but, because of the common natural association of pyrite and pentlandite, they are interpreted (Fig. 5) to include a divariant field of pns-pyrite (composition of pns 29.6–33.2 at. % Ni) sandwiched between two univariant assemblages, mss(1)-py-pn-v and py-mss(2)-pn-v. From the trends of the decrease in the Ni content of the pns coexisting with mss(2) and of the mss(1) coexisting with pns between 300°C and 230°C, it is estimated that pyrite-pentlandite tie lines are first established around 280°C, somewhat higher than the temperature (225 ± 25°C) reported by Craig and Naldrett (1971). At higher temperatures the extension of the mss prohibits equilibrium between pyrite and pentlandite.

Monoclinic pyrrhotite is considered a stable phase at 230°C (Fig. 5) on the basis of its stability in the Fe-S system below 292°C (Taylor, 1969) and the suggestion of Naldrett and Kullerud (1967) that the presence of Ni will not suppress the appearance of monoclinic pyrrhotite by more than 50°C. There are no systematic experimental data on the solid solution of Ni in monoclinic pyrrhotite. However the amount of Ni that can be accommodated in the ordered monoclinic structure is expected to be very restricted (5 wt % Ni in the range 300–260°C; unpublished data of Naldrett, 1966, cited in Naldrett and Kullerud, 1967), so that the extension of the mss(1) field to about 17 at. % Ni at 230°C prohibits tie lines between monoclinic pyrrhotite and pentlandite at this temperature. It is inferred that tie lines will not be established between these two phases until the mss(1) field has withdrawn to at least 10 at. % Ni, at some lower temperature.

Data from the present study suggest that some of the very Fe-rich (containing less than 5 at. % Ni) and Fe-poor (containing around 35.5 at. % Ni) mss phases have a M : S ratio higher than the 1 : 1 ratio of stoichiometric FeS, which is currently accepted as the metal-rich limit of the structure. This relative S deficiency of the mss has been supported by replicate analyses of several samples and by a more detailed

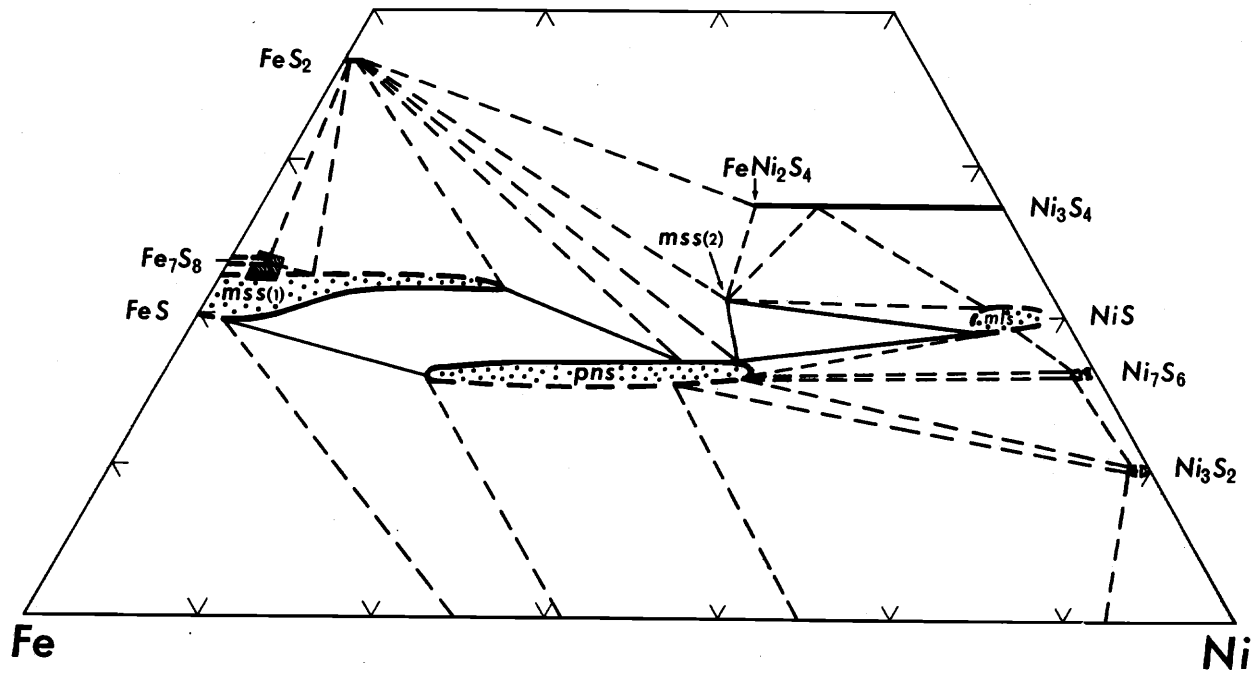

FIG. 5. Interpretive phase relations in the central portion of the condensed Fe-Ni-S system at 230°C. Hatched quadrilateral = bulk compositions of the Strathcona ore (Naldrett and Kullerud, 1967).

experimental investigation of the Fe-rich part of the boundary at 500°C (Table 4).

$(Ni,Fe)_7S_6$ solid solution: The present data on the gs phase is limited to the univariant assemblage gs-pns-mss-v at 600°, 500°, and 400°C which defines the Ni solubility limits of the pns field at these temperatures. Though the upper stability limit of the analogous αNi_7S_6 phase in the Ni-S system has been determined as 573°C (Kullerud and Yund, 1962), the gs phase is stabilized at some temperature above 600°C in the ternary system, presumably due to solid solution of Fe. The solubility of Fe in gs decreases with temperature, from 8.5 at. % at 600°C to a little less than 6 at. % at 400°C.

No attempt has been made to differentiate between α and $\beta(Ni,Fe)_7S_6$ in this work. In the binary system, the inversion to the high-temperature (αNi_7S_6) form is at about 400°C (Kullerud and Yund, 1962); so that all of the products actually analyzed may have been of $\alpha(Ni,Fe)_7S_6$.

$(Ni,Fe)_3S_2$ solid solution: Fields of hs at different temperatures have not been defined in the present study; only the compositions of hs in the univariant assemblage hs-pns-tn-v, which define the Fe solubility limit of hs at different temperatures, have been determined. The phase relations presented in the 600°C isothermal section (Fig. 1A) are slightly different from those of Naldrett et al. (1967) which show a univariant field of FeS-pns-hs-v and a divariant field of FeS-hs-v. At no temperature covered in the present study does the hs phase coexist with mss of any composition. The Fe solubility of this phase progressively decreases with decrease in temperature, from 11.3 at. % at 600°C to 2.9 at. % at 300°C. The Fe solubility limits determined in the present study are significantly higher than those estimated from the isothermal sections of Kullerud (1963b). The hs

TABLE 4. Compositions of Fe-Rich mss Synthesized at 500°C (Electron Probe Analyses)

Charge No.	Annealing Temp. (°C)	Annealing Time (Days)	Bulk Composition of Charge, Atomic % Fe	Ni	S	Composition of mss Phase, Atomic % Fe	Ni	S	Coexisting Phases Identified
KC-92	499	50	48.55	3.47	47.98	49.12	1.25	49.63	mss, tn
KC-93	499	50	47.51	3.87	48.62	47.85	2.08	50.07	mss, pns, tn
KC-94	499	50	46.37	4.45	49.18	47.92	2.17	49.91	mss, pns, tn
KC-104	500	36	46.66	3.34	50.00	47.32	2.63	50.05	mss, pns
KC-96	500	36	40.27	8.89	50.84	40.40	8.90	50.70	mss
KC-91	500	36	49.71	2.31	47.98	49.84	0.69	49.47	mss, tn

phase was identified in the material quenched from 600°C by X-ray powder diffraction. Therefore, in the absence of textural evidence indicating that it formed by inversion of the nonquenchable high temperature $(Ni,Fe)_{3\pm x}S_2$ phase (Kullerud and Yund, 1962), it appears that the addition of Fe increases the upper stability limit of Ni_3S_2 beyond 600°C.

Taenite: The tn (fcc Fe-Ni alloy) compositions determined fall into either of the two univariant assemblages: tn-pns-mss (Fe-rich)-v or tn-pns-hs-v (with the exception of the tn-pns-v divariant assemblage of KE-34). Because of the relative S-rich bulk compositions used in these experiments, tn is a subordinate phase in the two assemblages, but it is readily identified under the microscope by its high reflectivity, whitish-yellow color, and characteristic texture. The phase occurs either as thin, intergranular coatings or as small, spheroidal masses, sometimes showing a dendritic pattern of intergrowth. Electron probe analysis of the phase obtained in the low-temperature runs was very difficult because of the small size of the grains. Most of the present analyses of the phase indicate up to about 0.5 at. % S. On the basis of the extremely low solubility of S in Fe and Ni (a maximum of 0.06 at. % S; Lundqvist, 1947a,b), most of this S is probably due to contamination from the surrounding S-rich phases in the assemblages, though the possibility of minor amounts of S in solid solution in tn cannot be ruled out.

The tn coexisting with mss and pns shows a systematic variation in composition with temperature, from 63.8 at. % Ni at 600°C to 61.3 at. % Ni at 400°C, but a marked decrease in Ni content at lower temperatures (26.7 at. % at 285°C and 26.0 at. % at 230°C). The tn coexisting with pns and hs has a fairly uniform composition of about 72–73 at. % Ni (close to $FeNi_3$) down to 300°C and then shows a small decrease to 67.5 at. % Ni at 230°C. The phase was too fine-grained in the 230°C runs for electron probe analysis. and so the tn compositions in the 230°C runs have been estimated from their lattice parameters (Misra, 1972). However there is good evidence (discussed in the following section) that tn is relatively unreactive at temperatures below 400°C and that the above data do not represent equilibrium compositions for 285° and 230°C. The small shift in tn compositions from 600° to 400°C and the good agreement between the available natural data and that for 400°C suggests that the low-temperature composition range of tn coexisting with pns is probably similar to that for the 400°C isotherm, and this assumption is made in presenting the low-temperature phase relations (Figs. 1D, 1E, 5, and 7).

Statement of equilibrium

The present experimental investigation involved a departure from the standard procedure for silica tube experiments (Kullerud and Yoder, 1959) in that the starting compositions were melted and quenched before annealing. For this reason, some estimate of the attainment of equilibrium in our experiments and the general validity of the data presented above should be given.

The new technique was adopted because it was found in preliminary studies that the grain sizes of the annealed products obtained this way were large enough for electron probe analysis. Furthermore it was appreciated that because of the low vapor pressures of the metals at most of the temperatures investigated, homogenization of the phases would be effected by solid diffusion of the metal atoms, and that the reduction of the intergranular vapor space resulting from melting and quenching of the starting compositions would greatly facilitate this end. The common practice of interrupting annealing experiments to homogenize the charges by grinding not only tends to result in grain sizes too small for reliable electron probe analysis, but also does not appear to be as effective as the present technique in promoting the solid state reactions. It is felt that the reactivity observed in our low temperature experiments is a direct consequence of the new technique. The nature of the crystalline phases in the starting compositions before annealing were not investigated. However we would expect that solidification of the liquid and inversion of the nonquenchable phases would result in phases similar to those observed at 600°C, but that the compositions of these phases would be inhomogeneous as was obtained in the case of the charges quenched from 700°C (Fig. 4). Generally, then, annealing of the charges would simply involve homogenization of phases already present to equilibrium compositions and proportions, rather than reaction to produce new phases.

As in many experimental investigations, it is not possible to make an unequivocal statement of equilibrium to cover all of the products examined in this study. Some of the points favoring a close approach to equilibrium and steady-state conditions are as follows:

(1) The general features of the phase relations at moderate temperatures are consistent with the results of previous investigators and grade in a systematic manner down to the phase relations obtained at low temperatures.

(2) Complete homogenization of the phases is suggested in that compositional zoning and significant grain-to-grain variations in composition were not observed for any phase that occurred in grains large enough for accurate electron probe analysis. In addition the bulk compositions plot very close to the relevant tie lines in the divariant fields and within the three-phase areas of the univariant fields.

(3) Good agreement between the compositions of the coexisting phases has been obtained in several instances where different bulk compositions were used; for example, hs and pn compositions in KC-29 and 30, KD-32 and 33, KE-35 and 36; mss compositions in KC-28, 93 and 94; the mss and pns boundaries delineated by the charges KC-93, 94, 96, and 104 and the charges KC-10, 11, 13, and 28.

Annealing of charges KF-49 at 285°C and of KG-90 at 230°C produced a small amount of tn, coexisting with mss and pns: the tn appeared homogeneous with compositions of 26.7 and 26.0 at. % Ni, respectively. However the accepted phase data for the Fe-Ni system (Owen and Liu, 1949) indicate that, at these temperatures, alloys of these compositions should consist of coexisting taenite and kamacite. Moreover the composition of tn is significantly different from that at 400°C, and the reaction rates in the binary system are known to be very sluggish at temperatures below 500°C. We interpret the Fe-rich alloy composition to represent that of the tn formed from the melt before annealing. It can be established, then, that tn is unreactive in the low temperature experiments. The reactivity of each of the other phases will vary with its particular properties. However, our experiments have demonstrated that the mss phase is still relatively reactive at 230°C and the apparent homogeneity of it and of many of the coexisting phases is good evidence that a steady state has been realized.

Compositions of Natural Pentlandite Assemblages

Ternary pentlandite assemblages have been analyzed by the electron probe in samples from several sulfide deposits across Canada. Most of the samples were from the "Suffel Collection" of the Department of Geology, University of Western Ontario; Mr. J. Holland, Falconbridge Nickel Mines Ltd., provided some of the Falconbridge samples and Dr. N. D. MacRae, University of Western Ontario, lent samples 500 and 1351 (Fleet and MacRae, 1969). Only a few samples from each deposit have been analyzed so that the results are not claimed to be representative of the respective deposits. At the time this study was initiated, limited electron probe analyses of these phases had been published (Springer et al., 1964; Knop et al., 1965; Chamberlain et al., 1965; and Buchan and Blowes, 1968). Subsequently electron probe analyses of almost all the relevant phases have appeared (Vaughan, 1969; Kulagov et al., 1969; Graterol and Naldrett, 1971; Vaughan et al., 1971; Nickel, 1972; Naldrett et al., 1972; and Harris and Nickel, 1972). Pentlandite and pyrrhotite analyses from the present study are given in Table 5 and are compared with published data for these phases in Tables 6 and 7, respectively. Similar data for pyrite, bravoite, violarite, millerite, godlevskite, heazlewoodite, and awaruite are given in Table 8. The abbreviations for the mineral names used in this and the following sections are: aw = awaruite, gf = gersdorffite, gs = godlevskite, hpo = hexagonal pyrrhotite, hz = heazlewoodite, ml = millerite, mpo = monoclinic pyrrhotite, ms = marcasite, pm = polydymite, pn = pentlandite, po = pyrrhotite, py = pyrite, sph = sphalerite, tr = troilite, vl = violarite, vs = vaesite, bv = bravoite, cp = chalcopyrite.

Pentlandite: The textural varieties of pentlandite observed in polished sections of the Canadian samples are: (1) massive (blocky) pentlandite, often with islands and tiny inclusions of pyrrhotite; (2) rims of pentlandite partially or almost completely surrounding pyrrhotite grains; and (3) stringers, veinlets, and blebs of pentlandite, some of which are clearly oriented along the cleavage directions of the host pyrrhotite. The electron probe analyses show no systematic compositional differences among these different textural types of pentlandite.

The compositional data to date indicate that the solid solution limits of natural pentlandite extend from about 18.0 to 34.0 at. % Ni. As expected from the phase relations in the synthetic Fe-Ni-S system presented above, the composition of natural pentlandite is found to vary systematically with the assemblage; the Ni content of the pentlandite increases with increase in Ni content of the bulk composition of the sulfide assemblage (Fig. 6). This variation confirms the conclusions of Graterol and Naldrett (1971) and Harris and Nickel (1972). The spread of pentlandite compositions in assemblages like troilite-pentlandite, hexagonal pyrrhotite-monoclinic pyrrhotite-pentlandite, and millerite-pyrite-pentlandite possibly reflects differences in equilibration temperatures; however the extensive overlap of pentlandite compositions in the assemblage involving hexagonal pyrrhotite, monoclinic pyrrhotite, and pyrite is more suggestive of disequilibrium at low temperatures. The Co content of pentlandite is highly variable, the range being from an almost Co-free pentlandite with less than 0.1 at. % Co to an Fe-free pentlandite, $Co_{6.9}Ni_{1.3}S_8$, with 42.47 at. % Co (Petruk et al., 1969) and a Ni-free pentlandite, $Co_{9.1}Fe_{0.2}S_8$, with 52.60 at. % Co (Stumpfl and Clark, 1964). The solid solution between "normal" pentlandite, $(Fe, Ni)_9S_8$, and the isostructural cobalt-pentlandite, Co_9S_8 (Knop and Ibrahim, 1961; Geller, 1962), is readily interpreted as a process of substitution of Co for both Fe and Ni in the structure. Partition of the Co proportional to the Fe and Ni contents of pentlandites to give adjusted Ni contents (Ni* in Table 6) does not affect significantly the variation in pentlandite composition with assemblage.

The S contents of the pentlandites analyzed vary

TABLE 5. Average Composition of Natural Pyrrhotite Phases and Pentlandite (Electron Probe Analyses)

Sample Locality	Sample No.	Assemblage	Phase Analyzed	Composition, at. % Fe	Ni	Co	Cu	S
Beatty Twp., Ontario	500	tr,hpo,pn	tr	50.14	0.09	0.00	0.01	49.76
			hpo	47.81	0.14	0.00	0.02	52.03
			pn	28.49	24.30	0.79	0.00	46.42
Great Lakes Nickel, Ontario	1351	tr,hpo,pn	tr	49.76	0.12	0.00	0.01	50.11
			hpo	47.54	0.21	0.00	<0.01	52.25
			pn	27.76	25.00	0.55	0.00	46.69
Alexo, Ontario	6021	tr,hpo,pn	tr	49.72	0.12	0.00	0.04	50.12
			hpo	47.22	0.20	0.00	0.02	52.57
			pn	28.06	24.91	0.66	0.00	46.37
Frood, Sudbury	51	hpo,mpo,pn	hpo	45.56	0.68	0.00	0.04	52.72
			mpo	46.04	0.46	0.00	0.02	53.48
			pn	24.13	27.60	1.21	0.00	47.06
Falconbridge, Sudbury	52	hpo,mpo,pn	hpo	46.85	0.44	0.00	0.00	52.71
			mpo	45.86	0.46	0.00	0.00	53.68
			pn	24.70	27.88	0.37	0.00	47.05
Moak Lake, Manitoba	4706	hpo,mpo,pn	hpo	47.09	0.21	n.d.	n.d.	52.70
			mpo	46.08	0.19	n.d.	n.d.	53.73
			pn	26.61	27.05	0.60	0.00	45.74
Falconbridge, Sunbury	8	hpo,mpo,py,pn	hpo	46.98	0.51	0.10	0.01	52.40
			mpo	46.07	0.59	0.06	0.03	53.25
			pn	24.56	28.90	0.56	0.00	45.98
Lynn Lake ('A' ore body), Manitoba	3922	hpo,mpo,py,pn	hpo	47.24	0.72	0.00	<0.01	52.04
			mpo	45.49	0.65	0.00	0.01	53.85
			pn	23.69	28.82	0.99	0.00	46.50
Lynn Lake ('EL' ore body), Manitoba	6432	hpo,mpo,py,pn	hpo	47.30	0.34	0.00	0.01	52.35
			mpo	46.15	0.51	<0.01	0.01	53.33
			pn	24.50	28.44	0.83	0.00	46.23
Thompson Mine, Manitoba	8023	hpo,mpo,pn,pn	hpo	46.87	0.45	0.08	0.02	52.58
			mpo	46.02	0.52	0.09	0.02	53.35
			pn	24.77	28.56	0.18	0.05	46.44
Marbridge No. 1, Quebec	7076	hpo,mpo,py,pn	hpo	47.03	0.40	0.00	0.00	52.57
			mpo	46.13	0.34	0.00	0.00	53.53
			pn	24.87	27.81	0.32	0.00	47.00
Falconbridge, Sudbury	1	hpo,mpo,py,pn	hpo	46.93	0.34	0.11	0.00	52.62
			mpo	46.23	0.38	0.08	0.06	53.25
			pn	24.60	28.04	1.27	0.00	46.09
Falconbridge, Sudbury	2	hpo,mpo,py,pn	hpo	46.79	0.53	0.10	0.06	52.52
			mpo	45.93	0.72	0.12	0.02	53.21
			pn	24.32	28.55	0.56	0.00	46.57
Carson, Sudbury	3589	hpo,mpo,py,pn	hpo	47.18	0.31	0.00	0.01	52.50
			mpo	46.65	0.30	0.00	0.02	53.03
			pn	25.38	27.46	0.89	0.01	46.26
Marbridge No. 1, Quebec	6957	hpo,mpo,py,pn	hpo	47.31	0.27	0.00	0.00	52.42
			mpo	46.30	0.23	0.00	0.00	53.47
			pn	25.87	27.40	0.33	0.00	46.40
Paradee Twp., Ontario	6304	hpo,mpo,py,pn	hpo	46.66	0.65	0.05	0.00	52.64
			mpo	46.52	0.34	0.01	0.00	53.13
			pn	23.94	26.70	2.25	0.06	47.05
Lake Renzy, Quebec	545	hpo,mpo,py,pn	hpo	47.22	0.37	0.00	0.01	52.40
			pn	24.96	26.42	1.97	0.00	46.65
Strathcona, Sudbury	617	hpo,mpo,py,pn	hpo	46.77	0.47	n.d.	n.d.	52.76
			mpo	45.97	0.56	n.d.	n.d.	53.47
			pn	24.57	27.35	0.66	0.00	47.42

TABLE 5.—(*Continued*)

Sample Locality	Sample No.	Assemblage	Phase Analyzed	Composition, at. % Fe	Ni	Co	Cu	S
Creighton, Sudbury	9868	mpo,pn	mpo	46.01	0.62	0.00	<0.01	53.37
			pn	24.72	27.68	0.40	0.00	47.20
Falconbridge, Sudbury	4	mpo,pn	mpo	46.35	0.39	0.00	0.00	53.26
			pn	24.32	27.05	1.26	0.01	47.36
Stobie Open Pit, Sudbury	3878	mpo,py,pn	mpo	46.25	0.57	0.00	<0.01	53.18
			pn	24.08	28.23	0.95	0.01	46.73
Thompson Mine, Manitoba	5929	mpo,py,pn	mpo	46.28	0.38	0.00	0.01	53.33
			pn	24.76	27.73	0.07	0.00	47.44
Shebandowan, Ontario	11918	mpo,py,pn	mpo	46.55	0.37	0.00	0.00	53.08
			pn	24.47	28.41	0.41	0.00	46.71
Lord Brassey Mine, Tasmania	864	hz,ml,pn	pn	5.08	15.46	33.28	0.01	46.17
Texmont, Ontario	9635	hz,pn	pn	23.07	29.83	0.45	0.02	46.63

between 45.7 and 47.4 at. % S, two-thirds of the values being less than the ideal composition of 47.06 at. % S for stoichiometric M_9S_8. Thus most of the natural pentlandites seem to be relatively S-deficient, which agrees with the conclusion of Knop et al. (1965) and Harris and Nickel (1972), although the range of S variation found in this study is more restricted than that of the latter authors (45.7–48.5 at. % S); this may be due to the smaller number of samples analyzed in the present study. On the basis of the phase relations in the synthetic system, one would expect the pentlandites coexisting with heazle-

TABLE 6. Summary of Compositions of Natural Pentlandites (at. %) in Nickel Sulfide Assemblages (Ni and Co Data Only)

Assemblage	Ni	Co	Ni*	Source of Data
tr-aw-pn	No analytical data			
tr-pn	18.3–21.6	0.8– 4.9	19.8–22.4	Harris and Nickel (1972)
	22.6	0.7	22.9	Papunen (1970)
tr-hpo-pn	24.3–25.0	0.6– 0.8	24.7–25.3	Present study
	24.8	0.9	25.2	Graterol and Naldrett (1971)
	23.5–25.2	0.8– 1.0	24.0–25.7	Papunen (1970)
hpo-pn	Assemblage not reported			
hpo-mpo-pn	27.0–27.9	0.4– 1.2	27.4–28.2	Present study
	25.6–27.6	0.0– 0.9	26.0–27.6	Harris and Nickel (1972)
	27.2–28.6	0.3– 1.9	27.6–28.8	Vaughan et al. (1971)
mpo-pn	27.0–27.7	0.4– 1.3	27.7–27.9	Present study
	24.0–29.2	0.6– 5.0	24.9–29.8	Harris and Nickel (1972)
	25.0–27.3	0.2– 0.9	26.4–27.4	Papunen (1970)
mpo-py-pn	27.7–28.4	0.1– 1.0	27.8–28.7	Present study
	27.3–28.1	0.6– 1.8	27.6–29.1	Harris and Nickel (1972)
	27.4–28.2	0.2– 0.4	27.5–28.4	Graterol and Naldrett (1971)
py-pn	29.3–30.1	0.4– 0.8	29.5–30.6	Harris and Nickel (1972)
	30.1–32.4	0.2– 1.8	30.2–33.5	Graterol and Naldrett (1971)
py-ml-pn (-vl)	30.3–33.0	0.3– 1.1	30.5–33.4	Graterol and Naldrett (1971)
	33.3	0.2	33.4	Buchan and Blowes (1968)
ml-pn	No analytical data			
ml-hz-pn	15.5	33.3	40.5	Present study
	33.1–33.7	1.2– 4.2	34.5–34.9	Harris and Nickel (1972)
	33.8–34.2	0.9– 1.2	34.6–34.7	Graterol and Naldrett (1971)
ml-hz-pn (-gs)	33.8	0.8	34.3	Naldrett et al. (1972)
hz-pn	29.8	0.5	30.1	Present study
	24.3–24.9	9.3–10.4	29.4–30.9	Harris and Nickel (1972)
	9.8–26.7	11.4–41.7	33.6–46.6	Harris and Nickel (1972)
hz-aw-pn	No analytical data			
aw-pn	21.4–22.9	0.7– 3.6	22.0–23.8	Harris and Nickel (1972)
	16.8–19.1	20.7–29.3	31.2–37.1	Harris and Nickel (1972)
hpo-mpo-py-pn	26.4–28.9	0.2–2.2	27.7–29.4	Present study
	26.7–28.6	0.3–2.1	27.8–28.8	Vaughan et al. (1971)

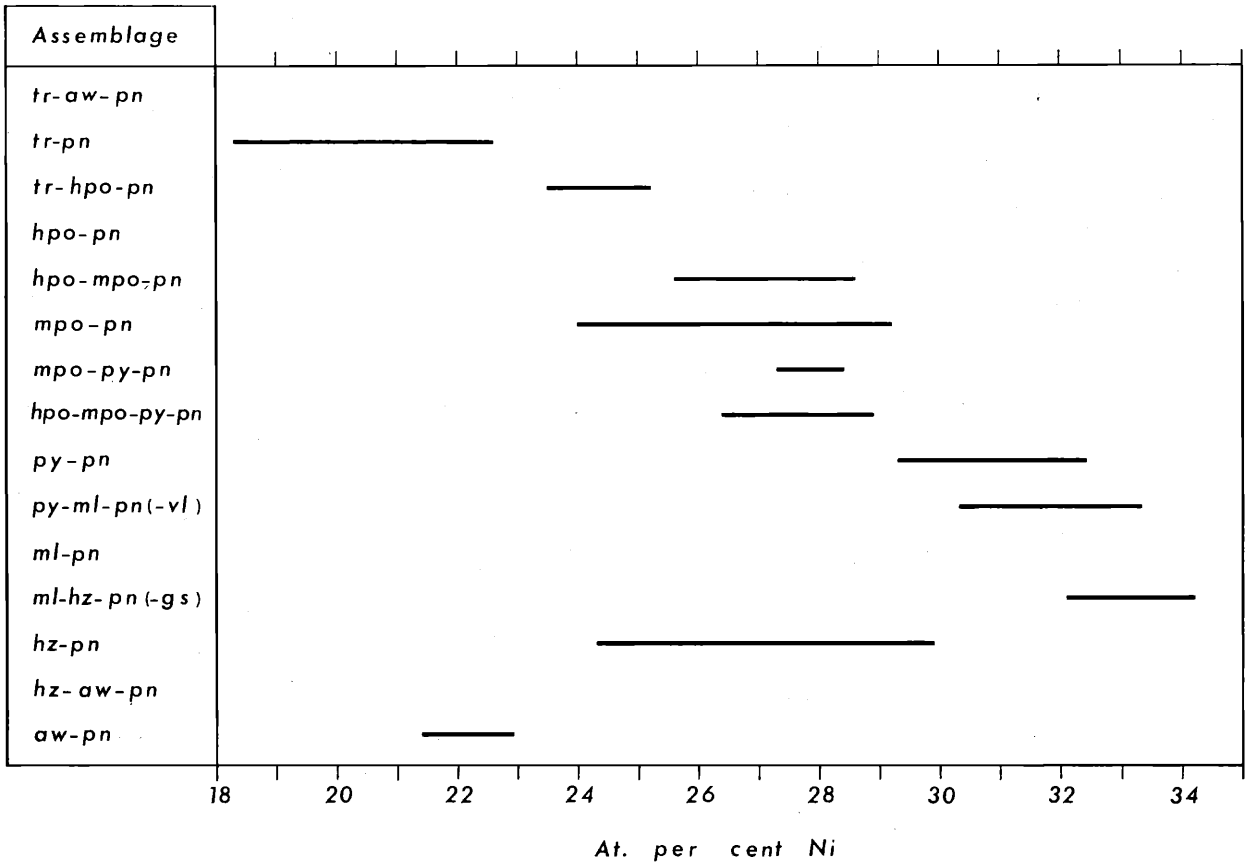

FIG. 6. Compositions of natural pentlandites in nickel sulfide assemblages. Data are from all sources; pentlandites with more than 10 at. % Co are not included; compositional data are not available for pentlandites in assemblages tr-aw-pn, hpo-pn, ml-pn, and hz-aw-pn.

woodite and/or awaruite to be relatively S-poor compared to those coexisting with pyrrhotite, pyrite, and millerite. However this correlation is not indicated by the analytical data.

Pyrrhotite: The pyrrhotites in the individual polished sections of the Canadian samples examined are single-phase aggregates of monoclinic pyrrhotite or two-phase mixtures of monoclinic pyrrhotite and

TABLE 7. Summary of Data on Pyrrhotite Compositions

Composition, at. %S Low Temperature Synthetic Pyrrhotites			
tr	hpo (S-rich limit)	mpo	Source of Data
50.0	52.60	53.27	Grønvold and Haraldsen (1952)
50.0	—	53.33	Gehlen (1963)
—	52.7	53.33	Desborough and Carpenter (1965)
—	—	53.2	Clark (1966b)
49.93–50.05	52.55	53.2 –53.65	Yund and Hall (1968, 1969)
50.0 –50.2	52.8 ± 0.10	53.2 –	Arnold (1969)
50.0	52.65 ± 0.10	53.25–53.33	Taylor (1969)
	Natural pyrrhotites		
tr	hpo	mpo	
—	—	53.30–53.55	Kullerud et al. (1963)
49.8 –50.2	52.2–53.0	53.1 –53.4	Carpenter and Desborough (1964)
50.0	52.5–53.8	53.3 –53.7	Clark (1966a)
50.0	51.9–52.5	53.3	Arnold (1967)
50.59	52.0–52.5	53.1 –53.6	Papunen (1970)
—	52.2–53.0	53.0 –53.7	Vaughan et al. (1971)
49.76–50.12	52.0–52.7	53.0 –53.9	Present study

(intermediate) hexagonal pyrrhotite or hexagonal pyrrhotite and troilite. Single-phase hexagonal pyrrhotite or single-phase troilite were not identified. The pyrrhotite phases were identified by a combination of the following techniques: (1) spot analysis with the electron probe, (2) etching with a solution of chromic acid in water, and (3) examination of Jagodzinski powder photographs, including semiquantitative determination of relative intensities of the 102 peaks (or their split equivalents in the case of monoclinic phases) with a Joyce-Loebl microdensitometer. In general it was not possible to differentiate between the hexagonal pyrrhotite and monoclinic pyrrhotite areas in two-phase samples of these phases at the time of analysis, so that the distinction between them in this study is based mainly on the discrimination of electron probe spot analyses.

All the pyrrhotites contain less than or about 1.0 at. % Ni, in agreement with the data of Papunen (1970), Vaughan et al. (1971), Graterol and Naldrett (1971), and Harris and Nickel (1972). Higher values reported in the literature (Naldrett, 1961) are invariably associated with bulk analyses of pyrrhotite concentrates and most probably reflect contamination by pentlandite.

The range of Ni contents of the hexagonal pyrrhotite (0.14–0.21 at. %) is similar to that for the coexisting troilite (0.10–0.12 at. %). The range of Ni contents of the coexisting hexagonal pyrrhotite (0.21–0.72 at. %) and monoclinic pyrrhotite (0.19–0.72 at. %) are also very similar but significantly higher than the data for the troilite-hexagonal pyrrhotite pairs. Thus Ni does not seem to show any distinct preference for any one phase in the coexisting pairs troilite-hexagonal pyrrhotite and hexagonal pyrrhotite-monoclinic pyrrhotite. However the data of Vaughan et al. (1971) and of Batt (1972) indicate a higher Ni in hexagonal pyrrhotite than in the coexisting monoclinic pyrrhotite.

The present data for the S contents of pyrrhotites coexisting with pentlandite agree very well with those for synthetic, binary pyrrhotites and for pyrrhotites from a variety of natural assemblages (Table 7).

Pyrite: The occurrence of pyrite in nickel sulfide deposits is restricted to the assemblages containing monoclinic pyrrhotite, or monoclinic and hexagonal pyrrhotites, or millerite, pentlandite being common to all of them except the rare pyrite-millerite assemblage. It is not found in assemblages containing troilite, awaruite, or heazlewoodite.

The available analyses (Table 8) indicate the Ni and Co contents of pyrite are highly variable, 0.00–4.61 at. % Ni and 0.00–1.68 at. % Co. Pyrites with up to 7 wt % Ni have been reported by Karup-Møller (1969) from English Lake, Manitoba, but these have not been included in Table 8 because of the lack of data regarding the other elements. The solubility of Ni in pyrite has not been determined at various temperatures. However, from the experiments of Clark and Kullerud (1963), one may anticipate about 1 wt % Ni in pyrites equilibrated at 143–148°C. The Ni contents of natural pyrites are generally less than 1.0 at. %, consistent with low temperature equilibration.

Bravoite: Bravoite is a rare mineral in nickel sulfide assemblages and has been reported only from three Canadian deposits: Shebandowan and Lorraine Mine (see Naldrett and Gasparrini, 1971) and English Lake (Karup-Møller, 1969). It shows highly variable Ni contents—ranging from less than 2 at. % ("nickelian pyrite") to a maximum of about 25 at. % (Ni-rich "bravoite"). Compositional zoning is very common and the variation in composition between the different zones (Vaughan, 1969) is of the same order as the variation between samples (Springer et al., 1964).

Violarite-polydymite: Polydymite (Ni_3S_4), the Ni-rich end member of the violarite solid solution, has been reported from Vermilion Mine (Clarke and Catlett, 1889), Levack Mine (Wandke and Hoffman, 1924) and, recently, from Shebandowan (Watkinson and Irvine, 1964), but, in the absence of confirming chemical or X-ray data, the identification of polydymite, which is optically very similar to bravoite and violarite, is open to question. The ideal formula for violarite is $FeNi_2S_4$, but in geologic literature violarite is often used for the Fe-rich members of violarite-polydymite solid solution series.

Violarite encountered in the present study (sample 6304) is exclusively associated with pentlandite, occurring along cracks and cleavages, and as pseudomorphs often containing islands of pentlandite. This association and texture is characteristic of almost all occurrences of violarite in nickel sulfide deposits and is strongly suggestive of alteration of pentlandite to violarite, probably due to the action of meteoric water (Lindgren and Davy, 1924; Sandefur, 1942; Dennen, 1943; Michener and Yates, 1944; Williams, 1958; Karup-Møller, 1969; Bird, 1969; Graterol and Naldrett, 1971). Natural violarites (Table 8) seem to be characterized by significant variations in their compositions and especially by a relative deficiency in Fe. However the violarite in sample 6304, which was inhomogeneous in respect to the Fe, Ni distribution, was relatively Fe-rich (17–23 at. % Fe, 18–27 at. %, 2 at. % Co, and 55–56 at. % S). This extended compositional range of violarite is supported by the report of a violarite-like ($Fe_{5.0}Ni_{4.0}S_{11.0}$) phase coexisting with a new Fe-Ni-S mineral of composition $Fe_{8.6}Ni_{0.4}S_{11.0}$, Ni-rich pyrite, and

TABLE 8. Compositions of Pyrite, Bravoite, Violarite, Millerite, Godlevskite, Heazlewoodite, and Awaruite in Natural Nickel Sulfide Assemblages

Locality (and Sample No.)	Assemblage	Phase Analyzed	Composition, at. % Fe	Ni	Co	Cu	S	Analytical Method*	Source of Data
Shebandowan (1918)	mpo-pn-py	py	33.32	0.00	0.96	0.00	65.72	1	Present study
Pardee Twp. (6304)	mpo-hpo-pn-py	py	32.25	0.00	1.05	0.00	66.70	1	Present study
Marbridge No. 1 (7076)	mpo-hpo-pn-py	py	32.97	0.16	0.48	0.00	66.39	1	Present study
Murray mine	po-cp-ms-py	py	30.61	3.18	n.d.	tr.	66.21	2	Walker (1894)
Worthington mine	po-pn-py	py	32.49	1.69	n.d.	n.d.	65.82	2	Walker (1915)
Dennison mine	cp-ms-gf-py	py	28.71	4.61	n.d.	0.00	66.68	2	Thomson and Allen (1939)
Mill Close mine	bv-cp-py	py	32.80	0.00	0.00	0.12	67.08	1	Vaughan (1969)**
	bv-py	py	31.42	0.95	0.00	0.00	67.63		
Jussi Orebody	mpo-pn-cp-py	py	31.54	0.07	1.68	0.01	66.71	1	Papunen (1970)
		py	33.46	0.12	0.51	n.d.	65.91		
		py	33.45	0.53	0.23	0.01	65.78		
Strathcona	hpo-mpo-pn-py	py	32.61	0.00	0.58	0.00	66.81	1	Vaughan et al. (1971)
		py	33.07	0.00	0.30	0.00	66.63		
Mechernich, Germany	Pb-Zn ore	py	28.57	3.14	tr.	1.85	66.44	2	Kalb and Meyer (1926)
Marbridge No. 3	po-pn-py	py	33.07	0.01	0.49	n.d.	66.43	1	Graterol and Naldrett (1971)
Zone I		py	32.75	0.17	0.80	n.d.	66.28		
Zone II	ml-pn-py	py	33.03	0.05	0.44	n.d.	66.48		
		py	31.80	0.01	0.52	n.d.	67.67		
		py	31.61	0.02	0.69	n.d.	67.68		
		py	32.06	0.11	0.63	n.d.	67.20		
		py	32.56	0.00	0.68	n.d.	66.76		
		py	32.67	0.00	0.78	n.d.	66.55		
		py	32.17	0.00	0.83	n.d.	67.00		
		py	31.76	0.06	0.46	n.d.	67.72		
Marbridge No. 4	(po)-pn-ml-py	py	32.21	0.02	0.65	n.d.	67.12	1	Graterol and Naldrett (1971)
		py	32.30	0.04	0.63	n.d.	67.03		
		py	32.51	0.10	0.76	n.d.	66.63		
		py	32.67	0.15	0.67	n.d.	66.51		
		py	32.61	0.58	0.58	n.d.	66.23		
		py	32.43	0.57	0.57	n.d.	66.43		
Minasraga, Peru	Vanadium ore	bv	21.36	12.57	n.d.	n.d.	66.07	2	Hillebrand (1907)
Alaskan deposits	pn-po-vl-bv	bv	14.86	16.95	n.d.	n.d.	68.19	2	Buddington (1924)**
Mechernich, Germany	Pb-Zn ore	bv	12.82	17.66	2.33	0.31	66.88	2	Kalb and Meyer (1926)
Maubach and Mechernich, Germany	Pb-Zn ore	bv	31.60	1.73	0.00	n.d.	66.67	1	Springer et al. (1964)†
		bv	28.48	3.47	1.38	n.d.	66.67		
		bv	29.17	4.16	0.00	n.d.	66.67		
		bv	27.79	5.54	0.00	n.d.	66.67		
		bv	25.70	7.63	0.00	n.d.	66.67		
		bv	23.62	9.71	0.00	n.d.	66.67		
		bv	22.58	10.75	0.00	n.d.	66.67		
		bv	21.20	12.13	0.00	n.d.	66.67		
		bv	19.12	14.21	0.00	n.d.	66.67		
		bv	6.64	14.21	12.48	n.d.	66.67		
		bv	17.38	15.95	0.00	n.d.	66.67		
		bv	16.00	16.64	0.69	n.d.	66.67		
		bv	14.61	18.72	0.00	n.d.	66.67		
		bv	12.18	18.72	2.43	n.d.	66.67		
		bv	12.88	19.41	1.04	n.d.	66.67		
		bv	7.68	23.57	2.08	n.d.	66.67		
		bv	8.72	24.61	0.00	n.d.	66.67		
Mill Close mine	Cp-py-bv	bv	21.65	11.16	0.96	n.d.	66.23	1	Vaughan (1969)**
Maubach, Germany	Pb-Zn ore	bv-Zone 10	9.68	18.20	10.03	n.d.	62.09	1	Vaughan (1969)**
		Zone 12	17.14	17.23	2.41	n.d.	63.22		
		Zone 2	18.14	15.93	1.46	n.d.	64.47		
		Zone 5	20.93	13.62	1.25	n.d.	64.20		
		Zone 8	20.12	10.17	0.00	n.d.	69.71		
		Zone 7	22.99	12.40	0.21	n.d.	64.40		
		Zone 3	20.53	13.60	1.39	n.d.	64.48		
		Zone 1	22.99	12.33	0.28	n.d.	64.40		
		Zone 9	20.85	13.20	0.14	n.d.	65.81		
		Zone 11	24.48	7.44	0.82	n.d.	67.26		
		Zone 13	34.57	0.07	0.00	n.d.	65.36		
Cobalt, Ontario (Langis mine)	py-ms-pn-cp-sph-bv and arsenides	bv	0.75	7.64	26.52	n.d.	65.09	1	Petruk et al. (1969)
		bv	4.11	4.63	26.88	n.d.	64.38		
Vermilion mine	No data	vl	12.03	31.95	n.d.	n.d.	56.02	2	Clarke and Catlett (1889)
Vermilion mine	ml-vl	vl	12.78	29.33	0.79	n.d.	57.10	2	Short and Shannon (1930)
Julian, California	po-py-pn-vl	vl	14.66	25.70	1.89	n.d.	57.75	2	Short and Shannon (1930)

TABLE 8.—(*Continued*)

Locality (and Sample No.)	Assemblage	Phase Analyzed	Composition, at. % Fe	Ni	Co	Cu	S	Analytical Method*	Source of Data
Marbridge No. 2	ml-py-pn-vl	vl Gray	7.35	36.88	0.18	n.d.	55.59	1	Buchan and Blowes (1968)
		vl Pink	16.32	27.59	0.32	n.d.	55.77		
		vl Lavender	5.92	34.67	5.01	n.d.	54.40		
Marbridge No. 3, Zone II	ml-py-pn-vl	vl	12.26	34.74	0.56	n.d.	52.44	1	Graterol and Naldrett (1971)
		vl	9.70	34.13	0.83	n.d.	55.34		
		vl	10.81	34.21	0.89	n.d.	54.09		
		vl	9.64	33.86	0.50	n.d.	56.00		
Lord Brassey mine (864)	pn-hz-ml	ml	0.02	51.89	0.05	0.05	47.99	1	Present study
Noril'sk	pn-hz-ml-gs	ml	1.60	45.68	0.46	n.d.	52.26	1	Kulagov et al. (1969)
Texmont mine	pn-hz-ml-gs	ml	0.61	49.51	0.15	n.d.	49.73	1	Naldrett et al. (1972)
Marbridge No. 2	pn-py-ml-vl	ml	0.98	49.67	0.02	n.d.	49.33	1	Buchan and Blowes (1968)
Marbridge No. 3, Zone II	pn-py-ml-vl	ml	1.39	49.39	0.22	n.d.	49.00	1	Graterol and Naldrett (1971)
		ml	0.95	49.18	0.63	n.d.	49.24		
		ml	1.07	47.91	0.32	n.d.	50.70		
		ml	1.57	48.37	0.26	n.d.	49.80		
		ml	0.96	48.50	0.37	n.d.	50.17		
		ml	0.70	48.17	0.46	n.d.	50.67		
		ml	0.74	48.06	0.59	n.d.	50.61		
		ml	0.76	48.67	0.50	n.d.	50.07		
Marbridge No. 4	pn-py-ml	ml	1.40	48.55	0.25	n.d.	49.80	1	Graterol and Naldrett (1971)
		ml	1.00	49.80	0.64	n.d.	48.56		
Northern end of Jussi Orebody, Kotalahti	py-cp-ml	ml	0.23	51.72	0.25	0.09	47.71	1	Papunen (1970)
		ml	0.44	47.85	0.27	0.05	51.39		
Texmont	pn-ml-hz-gs	gs	3.03	50.24	0.06	n.d.	46.67	1	Naldrett et al. (1972)
Noril'sk	pn-ml-hz-gs	gs	2.44	47.55	0.46	n.d.	49.55	1	Kulagov et al. (1969)
Lord Brassey mine (864)	pn-ml-hz	hz	0.04	60.77	0.20	0.03	38.96	1	Present study
Texmont	pn-ml-hz	hz	0.22	59.90	0.00	n.d.	39.88	1	Graterol and Naldrett (1971)
Marbridge No. 3, Zone III	pn-ml-hz	hz	0.66	59.85	0.23	n.d.	39.26	1	Graterol and Naldrett (1971)
		hz	0.82	58.58	0.19	n.d.	40.41		
Texmont	pn-ml-hz(-gs)	hz	0.17	60.15	0.00	n.d.	39.68	1	Naldrett et al. (1972)
Noril'sk	pn-ml-hz(-gs)	hz	n.d.	56.03	n.d.	n.d.	43.97	1	Kulagov et al. (1969)
Eastern Twp.	associated with	aw	26.22	69.51	3.98	0.29	n.d.	2	Nickel (1959)
	silicates (-hz?)	aw	26.36	70.63	2.83	0.18	n.d.		
Muskox Intrusion	tr-pn-aw	aw	38.17	61.83	n.d.	n.d.	0.00	1	Chamberlain (1967); Chamberlain et al. (1965)
Lord Brassey mine, Tasmania	hz-aw	aw	23.90	76.10	n.d.	n.d.	n.d.	3	Williams (1960)
			−18.75	−81.25					
Awarua Bay, New Zealand	hz-aw	aw	28.35	68.92	2.73	n.d.	n.d.	2	Williams (1960)
Barn Bay, New Zealand	No data	aw	32.18	66.73	0.69	n.d.	0.40	2	Ulrich (1890)

* 1—Electron probe; 2—Wet chemical; 3—X-ray diffraction.
** S by difference.
† Estimated from the FeS_2-NiS_2-CoS_2 plot of the compositions.

chalcopyrite in eclogite nodules (Desborough and Czamanske, in press).

Millerite: The analyses of natural millerite show contents of 0.02–1.57 at. % Fe, 0.2–0.6 at. % Co, and less than 0.1 at. % Cu, so that the total amount of foreign metals in solid solution in millerite is of the order of 1.5 at. %. The S content of millerite ranges from 47.7 to 50.7 at. %. About 60% of the values fall below the stoichiometric proportion of 50.0 at. % S for NiS, suggesting that, as in the synthetic system, natural millerite tends to have a M : S ratio slightly greater than unity. The analyses of millerite, godlevskite, and heazlewoodite of Kulagov et al. (1969) are each significantly higher in S than the expected values, suggesting a consistent error in the determinative method, and these data have not been included in the discussion.

Godlevskite: Godlevskite, the mineral equivalent of βNi_7S_6, was first reported from the Noril'sk and Talnakh deposits of U.S.S.R. (Kulagov et al., 1969). Recently this mineral has been described from one sample of drill core from an unknown location in the Texmont mine (Naldrett et al., 1972). In both cases the Fe-Ni-sulfides associated with godlevskite has a S content very close to the ideal stoichiometric M_7S_6 composition. Both analyses (Table 8) show significantly higher Fe : Ni ratios than in either millerites or heazlewoodites.

Heazlewoodite: Although heazlewoodite has been found in association with most Ni-rich minerals (Table 9), compositional data are available for only the most common of the heazlewoodite-bearing assemblages, millerite - heazlewoodite - pentlandite (± godlevskite). The combined proportion of Fe, Co, and Cu in solid solution in heazlewoodite does not usually exceed 1.0 at. % (Table 8). The S con-

TABLE 9. Natural Occurrences of Phase Assemblages Shown in Figure 7

No.	Assemblage	Example(s) of Natural Occurrence(s)	Source of Data
1.	tr-aw-pn	Muskox Intrusion (native metal zone)	Chamberlain et al. (1965; Chamberlain (1967)
2.	tr-pn	Pefkos, Mooihock, Del Norte'Co., Muskox Intrusion	Harris and Nickel (1972)
		Hitura (Finland)	Papunen (1970)
3.	tr-hpo-pn	Alexo, Great Lakes Nickel, Beatty Twp.	Present study
		Alexo	Graterol and Naldrett (1971)
		Kotalahti & Hitura (Finland)	Papunen (1970)
4.	hpo-pn	Not reported	
5.	hpo-mpo-pn	Falconbridge, Frood, Moak Lake	Present study
		Old Nick, Expo Ungava	Harris and Nickel (1972)
		Strathcona	Vaughan et al. (1971)
6.	mpo-pn	Falconbridge, Creighton	Present study
		Muskox Intrusion, Dumbarton, Creighton, Strathcona, McKim, Falconbridge	Harris and Nickel (1972)
		Kotalahti & Hitura (Finland)	Papunen (1970)
7.	mpo-py-pn	Stobie, Thompson, Shebandowan	Present study
		Texmont D, Long Lac Rainy River	Harris and Nickel (1972)
		Marbridge No. 3 (Zone 1)	Graterol and Naldrett (1971)
8.	py-pn	Texmont A and C	Harris and Nickel (1972)
		Marbridge No. 4	Graterol and Naldrett (1971)
9.	py-ml-pn	Marbridge No. 3 (Zone II) & Marbridge No. 4	Graterol and Naldrett (1971)
		Marbridge No. 2	Buchan and Blowes (1968)
10.	ml-py	North end of Jussi orebody, Kotalahti (Finland)	Papunen (1970)
		Nickel Reward orebody (Tasmania)	Williams (1958)
11.	ml-py-vl	Not reported	
12.	py-vl	Not reported	
13.	py-vs	Locality not specified	Clark and Kullerud (1963)
14.	py-vs-vl	Not reported	
15.	vs-vl	Not reported	
16.	ml-vl	Vermilion Mine	Short and Shannon (1930)
17.	ml-pn	Not reported (pn-ml intergrowth common)	
18.	ml-hz-pn	Lord Brassey Mine (Tasmania)	Present study
		Helen, Texmont	Harris and Nickel (1972)
		Texmont	Naldrett et al. (1972)
		Noril'sk (U.S.S.R.)	Kulagov et al. (1969)
		Lord Brassey Mine and Trial Harbour Mine (Tasmania)	Williams (1958)
19.	hz-ml	Amos	Eckstrand (1971)
20.	hz-pn	Texmont	Present study
		Univex, Cassiar	Harris and Nickel (1972)
		Alexo	Naldrett (1967)
21.	hz-aw	Amos	Eckstrand (1971)
		Eastern Twp. (?)	Chamberlain (1966)
		Lord Brassey Mine (Tasmania)	Williams (1960)
22.	hz-aw-pn	Trial Harbour Mine (Tasmania)	Ramdohr (1950)
23.	aw-pn	Dumont	Harris and Nickel (1972)
		Amos	Eckstrand (1971)

tent of the heazlewoodite in sample 864 was found to be consistently between 38 and 39 at. %, indicating a relative S deficiency compared to M_3S_2. In contrast the analyses of Graterol and Naldrett (1971), with an analytical accuracy of $\pm$ 0.8 wt % S, suggest that the M : S ratio in natural heazlewoodite is very close to 3 : 2, in agreement with the data from synthetic studies in the Ni-S system (Kullerud and Yund, 1962).

Awaruite: In recent geological usage, the name "awaruite" has been applied to all terrestrial Fe-Ni alloys irrespective of the composition (the Fe-Ni alloy phases obtained in the synthetic system have been referred to as "taenite"). It is typically associated with serpentinized peridotite and is relatively rare in nickel sulfide assemblages. However awaruite has been reported in nickel sulfide assemblages in association with troilite-pentlandite, pentlandite, pentlandite-heazlewoodite, and heazlewoodite (Table 9). All these assemblages are in accord with the expected phase relations at low temperatures. Available analyses of the phase (Table 8) show that awaruite coexisting with heazlewoodite only is distinctly richer in Ni (about 70–80 at. % Ni) than that coexisting with troilite-pentlandite (about 62 at. % Ni).

Low Temperature Phase Relations

The above survey of the natural compositional data and various experiments involving the addition of components to selected parts of the ternary system by earlier workers supports the use of the Fe-Ni-S system to represent the phase relations of natural nickel sulfide assemblages. An interpretive phase diagram (Fig. 7) has been prepared in the light of the experimental and compositional data discussed

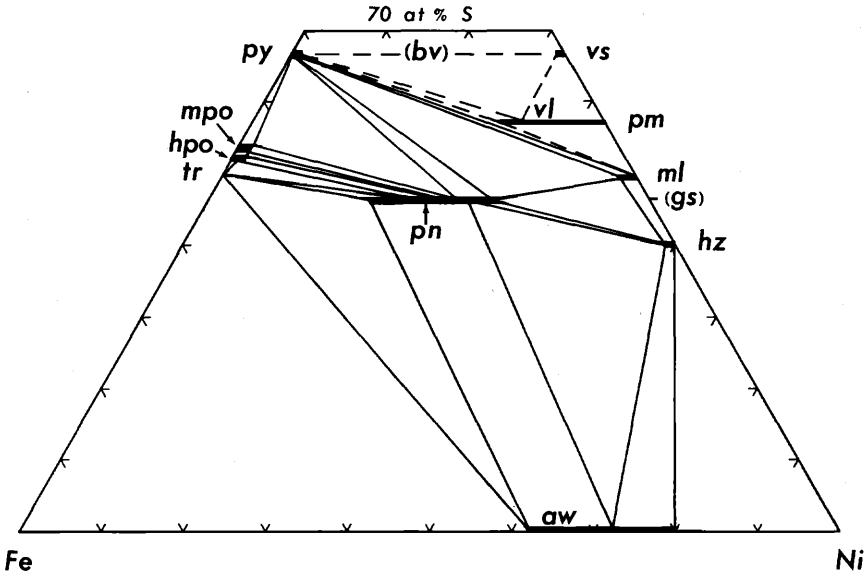

FIG. 7. Interpretive low-temperature phase diagram for the Fe-Ni-S system.

above, and essentially represents the present status of a diagram that has evolved over the last 25 years (Lundqvist, 1947a; Shewman, 1966; Kullerud et al., 1969; Graterol and Naldrett, 1971). There are several features of nickel sulfide assemblages strongly suggestive that, even though many features of them may have formed at moderate geological temperatures, they have continued to re-equilibrate after ore genesis at temperatures considerably lower than the lowest temperatures investigated experimentally: the most striking evidence for this is the low Ni contents of the pyrrhotite and pyrite and the low Fe contents of the millerite and heazlewoodite. Clearly the reactivity of the Fe-Ni-S phases at low temperatures will vary from mineral to mineral and we would expect specific minerals to readjust chemically without necessarily equilibrating with other phases in the assemblages, for example, the replacement of pentlandite by violarite and the segregation of troilite and hexagonal pyrrhotite from earlier formed pyrrhotite grains of intermediate composition. The phase diagram presented, then, represents the low temperature phase relations; the temperature associated with it (140°C) is partly artificial in that it allows for the presence of troilite but not of smythite, thought stable below 85°C (Taylor, 1969), while it is appreciated that, in reality, the chemical readjustment of specific minerals within the different assemblages might be arrested at temperatures outside this range. Examples of natural occurrences of the different assemblages represented in the phase diagram are given in Table 9 and more detailed discussion of these is given below.

The Ni-poor limit of the pentlandite field will be defined by the limiting composition of pentlandite in the assemblage troilite-pentlandite; the present data suggest that this is 20.0 at. % Ni* (Ni* is the co-adjusted Ni content). This is slightly higher than the composition of pentlandite (15 at. % Ni) obtained in the synthetic assemblage pn-mss(1)-aw at 230°C. The compositional range of pentlandite coexisting with troilite is quite extensive (20–23 at. %), but the implication from this, different temperatures of equilibration or disequilibrium, can be decided only by detailed study of individual specimens.

The average S contents of the hexagonal pyrrhotites analyzed in the present study—52.3 at. % with troilite and pentlandite, 52.7 at. % with monoclinic pyrrhotite and pentlandite, and 52.5 at. % with monoclinic pyrrhotite, pentlandite and pyrite—suggest a narrow compositional field for this phase and may account for the absence of documented hexagonal pyrrhotite-pentlandite assemblages. The common assemblage hexagonal pyrrhotite-monoclinic pyrrhotite-pyrite-pentlandite must reflect disequilibrium in the ternary system; whether hexagonal pyrrhotite or pyrite is the metastable phase may be estimated from the bulk, ternary composition. However for the Strathcona ores (Naldrett and Kullerud, 1967), the estimated bulk, ternary composition straddles the stability fields in question so that the metastability problem is indeterminate using this criterion. However the phase chemistry (Fig. 5) does show that, for these ores, the monoclinic pyrrhotite must have formed earlier than the pentlandite, if the latter formed by exsolution from mss and could not have

formed during the exsolution of pentlandite as has been suggested for some of the other Sudbury deposits. It has been noted that the Ni contents of coexisting troilite-hexagonal pyrrhotite is lower than that of coexisting hexagonal pyrrhotite-monoclinic pyrrhotite. If the Ni content of the former pair were established during the last major chemical event in these grains, during segregation of the phases, the inference is that the hexagonal pyrrhotite-monoclinic pyrhotite pair established final equilibrium somewhat above 140°C.

Because of the overlap in compositions of pentlandite in the natural assemblages hexagonal pyrrhotite-monoclinic pyrrhotite-pentlandite and monoclinic pyrrhotite-pentlandite, compositional limits of pentlandite shown for these assemblages in Figure 7 are arbitrary. Pentlandite in the natural pyrite-pentlandite assemblage shows 29.5 at. % Ni*. This correlates very well with the composition of pentlandite (about 29.5 to 33 at. % Ni) that would coexist with pyrite in the synthetic assemblage at 230°C (Fig. 5).

The phase diagram allows for the assemblages pyrite-millerite-pentlandite (Graterol and Naldrett, 1971) and pyrite-millerite (Williams, 1958; Papunen, 1970). It would be expected that pyrite coexisting with monoclinic pyrrhotite-pentlandite should be lower in Ni* than pyrite coexisting with millerite-pentlandite or millerite alone. This correlation is not apparent in the available compositional data. However, millerite in the millerite-pyrite assemblage from Finland (Papunen, 1970) does have a distinctly lower combined Fe and Co content than millerite in the pyrite-millerite-pentlandite assemblage.

Although pentlandite-millerite intergrowths are fairly common in nickel sulfide ores, we are not aware of any reported occurrence of an exclusive millerite-pentlandite assemblage. However, this assemblage was obtained in the synthetic system at 230°C, giving a pentlandite composition of about 34 at. % Ni.

Excluding the high-Co pentlandite from Tasmania (sample 864), the compositions of pentlandites in the natural assemblage millerite-heazlewoodite-pentlandite (± godlevskite), which defines the maximum Ni-solubility limit of the pns field, fall within the narrow range 34.5–34.9 at. % Ni*. The phase relations of βNi_7S_6 have not been investigated in the ternary system below 400°C, but in the binary system it is stable down to at least 200°C (Kullerud and Yund, 1962). However, the godlevskite in the Noril'sk specimens shows all stages of replacement by millerite (Kulagov et al., 1969) and, in the Texmont assemblage, it contains heazlewoodite veinlets. This textural evidence and the common occurrence of the assemblage pentlandite-millerite-heazlewoodite suggest that it is unstable at low temperatures and, accordingly, it has not been included as a stable phase in Figure 7.

The heazlewoodite-awaruite-pentlandite assemblage, stable in the synthetic system down to 230°C, has been reported only from Trial Harbour Mine, Tasmania (Ramdohr, 1950). However microscopic impregnations of heazlewoodite and awaruite are usually so fine-grained that misidentification can be avoided only if comparative material is available for study (Ramdohr, 1967), and it is possible that some of the natural heazlewoodite-pentlandite assemblages also contain awaruite which has escaped identification. In absence of analytical data for the awaruite in the natural heazlewoodite-awaruite-pentlandite assemblage, the composition of awaruite in this assemblage has been assumed to be about 73 at. % Ni, which is the composition of the corresponding synthetic phase in this assemblage at 400°C. The assemblage heazlewood-awaruite has been identified at Amos (Eckstrand, 1971) and Lord Brassey Mine, Tasmania (Williams, 1960). The Ni-rich limit of awaruite in this assemblage is taken to be approximately 80 at. % Ni on the basis of compositional data given by Williams (1960). The awaruite coexisting with pyrrhotite-pentlandite in the Muskox Intrusion (Chamberlain et al., 1965) shows about 62 at. % Ni. This is close to the expected composition of taenite coexisting with mss and pentlandite at low temperatures in the synthetic system.

We are not aware of any reported occurrence of the assemblages violarite-bravoite or violarite-bravoite-vaesite, nor have such assemblages been demonstrated experimentally. A secondary assemblage violarite-bravoite-nickeliferous pyrite (with marcasite and primary low-Ni pyrite) has been reported from English Lake, but both the bravoite, containing 11 to 12 wt % Ni and occurring mostly as a matrix for, and as zones in, idiomorphic secondary pyrite crystals, and the nickeliferous pyrite, containing up to 7 wt % Ni, have been interpreted as metastable phases in this assemblage (Karup-Møller, 1969). Therefore, the phase relations involving bravoite, as shown by Graterol and Naldrett (1971), do not seem justified. On the other hand the spread in compositions of natural bravoites from different localities and between the zones of a single grain (Table 9) and the possibility that the bravoite synthesized by Clark and Kullerud (1963) was actually a metastable phase (Shimazaki, 1971) suggest the existence of a metastable solid solution $FeS_2 = NiS_2 (-CoS_2)$ at low temperatures. Vaesite is a rare mineral and has not been reported from nickel sulfide assemblages, but where found in nature, it occurs with pyrite (Clark and Kullerud, 1963; these authors cite one exception from Missouri where vaesite occurs with bravoite). Thus pyrite-vaesite appears to be the stable assem-

blage at low temperatures. The assemblages pyrite-vaesite-violarite and vaesite-violarite shown in Figure 7 are entirely interpretive since their existence has not been documented, either in the field or in the laboratory.

Summary

The phase relations of pentlandite assemblages in the Fe-Ni-S system have been reinvestigated at 600°, 500°, 400°, 300°, and 230°C. The work used modifications of the accepted procedure for studying sulfide phase relations in sealed, silica tube, annealing experiments, in that the charges were melted and quenched before annealing, and the quenched products of the annealing experiments were analyzed with an electron probe. The principal findings from this part of the study are:

1. The phase boundaries are located with much greater accuracy than in previous work and actual tie lines plotted.

2. The variations in the solid solution limits of pentlandite with temperature are asymmetrical and somewhat unsystematic. The Fe solubility limit progressively increases with decrease in temperature, from 33 at. % Fe at 600°C to a maximum of 40 at. % Fe at 285°C, and then decreases with falling temperature to 30 at. % at 230°C. The Ni solubility limit of the pentlandite solid solution (pns) field reaches a maximum of about 41 at. % Ni at 600°C and a minimum of 34 at. % Ni at 300°C. Most compositions in the pns field are deficient in S relative to the stoichiometric composition.

3. The S-poor boundary of the monosulfide solid solution (mss) field recedes progressively toward S-rich compositions with falling temperature. The S limits of the boundary at a section with atomic Fe: Ni ratio 1 : 1 are estimated as 50.7, 51.0, 51.3, and 51.8 at. % S at 600°, 500°, 400°, and 300°, respectively. The boundary does not extend up to this section at 230°C.

4. The mss field, which is continuous between $Fe_{1-x}S$ $Ni_{1-x}S$ at higher temperatures, separates into two immiscible mss phases, mss(1) and mss(2), below 400°C. The breakdown occurs at the composition of about 33 at. % Ni, which is correlated to both a change in the slope of mss-pns tie lines and a discontinuity in the c-parameter, composition curve. The mss(1) phase withdraws progressively toward the Fe-S join with falling temperature, while the composition of the mss(2) phase is stabilized around 33 at. % Ni. This phase is presumed to be unstable at lower temperatures since a mineral of corresponding composition has not been reported to date.

5. It is estimated that tie lines between pyrite and pentlandite are established at about 280°C.

6. Some of the very Fe-rich (containing less than 5 at. % Ni) and Fe-poor (in the range of about 36–40 at. % Ni) mss phases have an atomic M : S ratio higher than the 1 : 1 ratio of stoichiometric FeS.

7. The thermal stability of the $\alpha(Ni,Fe)_7S_6$ phase is increased because of Fe in solid solution, so that the phase appears in the Fe-Ni-S system at a higher temperature (above 600°C) than in the Ni-S system. The solubility of Fe in this phase decreases with falling temperature, from about 8.5 at. % Fe at 600°C to about 6 at. % at 400°C.

8. The solubility of Fe in the $(Ni,Fe)_3S_2$ solid solution (hs) decreases with falling temperature, from 11 at. % Fe at 600°C to 3 at. % Fe at 300°C. The composition of this phase is believed to be close to Ni_3S_2 at lower temperatures.

9. The compositions of taenite (tn) in the univariant assemblages tn-pns-mss and tn-pns-hs at 400°C are 61 and 73 at. % Ni, respectively. The compositions of taenite in the corresponding assemblages at low temperature are thought to be similar to these data.

Compositional data on natural pentlandite assemblages from the present work and from the literature are compared. The Ni content of pentlandite varies systematically with the assemblage, the data to date indicating limits of 18 at. % Ni when coexisting with troilite and 34 at. % Ni when coexisting with heazlewoodite and millerite. The Co content is highly variable from less than 0.1 at. % to about 33 at. %. Most pentlandites contain less than the stoichiometric amount of S, although a systematic variation of the S content with assemblage is not indicated. Pyrrhotite generally contains less than 1 at. % Ni. The data from the present work suggest that the Ni contents of coexisting troilite-hexagonal pyrrhotite are significantly lower than those of coexisting hexagonal pyrrhotite-monoclinic pyrrhotite.

Synthesis of the present experimental data and of the data on the nature and compositions of phases in natural pentlandite assemblages permits statements to be made on the stability of the natural phases:

1. The natural assemblages have continued to readjust chemically after ore genesis at temperatures considerably lower than the lowest temperature investigated experimentally (230°C). The most emphatic evidence for this are the low Ni contents of pyrrhotite and pyrite and the low Fe contents of millerite and heazlewoodite.

2. The lower Ni contents of coexisting troilite-hexagonal pyrrhotite over those of coexisting hexagonal pyrrhotite-monoclinic pyrrhotite is indicative of a lower temperature of final readjustment for the former minerals.

3. The common assemblage hexagonal pyrrhotite-monoclinic pyrrhotite-pyrite-pentlandite must contain one metastable phase.

4. Monoclinic pyrrhotite must form earlier than pentlandite from bulk compositions similar to the Strathcona ores and the exsolution of the pentlandite from the mss in these ores initiated at temperatures significantly lower than 230°C.

5. The limits of solid solution of Ni in natural pentlandites (18 and 34 at. %) are similar to those obtained in low temperature synthetic pentlandites.

6. The limiting natural compositions of awaruite coexisting with pentlandite correlate with the equivalent data for the low-temperature synthetic system.

In conclusion, then, this work has strengthened the contention that crystal-crystal equilibria have been the principal factors controlling the phase chemistry and compositions of natural nickel sulfide assemblages. The good agreement between several limiting compositions in comparing the synthetic and natural data is very encouraging, suggesting that the factors ignored in making the comparisons, hydrostatic pressure, possible mobile components, and other chemical components, are, perhaps, not all that significant.

Acknowledgments

This work was supported by an N.R.C. operating grant. Professors G. G. Suffel and N. D. MacRae, University of Western Ontario, and J. Holland, Falconbridge Nickel Mines Ltd., kindly provided natural samples.

Department of Geology
University of Western Ontario
London, Ontario, Canada

REFERENCES

Arnold, R. G., 1967, Range in composition and structure of 82 natural terrestrial pyrrhotites: Canadian Mineralogist, v. 9, p. 31–50.

—— 1969, Pyrrhotite phase relations below 304 ± 6°C at 1 atm. total pressure: Econ. Geol., v. 64, p. 405–419.

Batt, A. P., 1972, Nickel distribution in hexagonal and monoclinic pyrrhotite: Canadian Mineralogist, v. 11, p. 892–897.

Bird, W. H., 1969, A note on the occurrence of violarite, Copper King mine, Boulder County, Colorado: Econ. Geol., v. 64, p. 91–95.

Buchan, R., and Blowes, J. H., 1968, Geology and mineralogy of a millerite nickel ore deposit: Canadian Mining Metall. Bull., v. 61, no. 672, p. 529–534.

Buddington, A. F., 1924, Alaskan nickel minerals: Econ. Geol., v. 19, p. 521–541.

Carpenter, R. H., and Desborough, G. A., 1964, Range in solid solution and structure of naturally occurring troilite and pyrrhotite: Am. Mineralogist, v. 49, p. 1350–1365.

Chamberlain, J. A., 1966, Heazlewoodite and awaruite in serpentinites of the Eastern Townships, Quebec: Canadian Mineralogist, v. 8, p. 519–522.

—— 1967, Sulphides in the Muskox intrusion: Canadian Jour. Earth Sci., v. 4, p. 105–153.

—— McLeod, C. R., Traill, R. J., and Lachance, G. R., 1965, Native metals in the Muskox intrusion: Canadian Jour. Earth Sci., v. 2, p. 188–215.

Clark, A. H., 1966a, The mineralogy and geochemistry of the Ylöjärvi Cu-W deposits, southwest Finland: Mackinawite-pyrrhotite-troilite assemblages: Soc. Géol. Finlande Comptes rendus., no. 37, p. 195–199.

—— 1966b, Stability field of monoclinic pyrrhotites: Inst. Mining Metallurgy Trans., v. 75, sec. B, p. 232–235.

Clark, L. A., and Kullerud, G., 1963, The sulfur-rich portion of the Fe-Ni-S system: Econ. Geol., v. 58, p. 853–885.

Clarke, F. W., and Catlett, C., 1889, A platiniferous nickel ore from Canada: Am. Jour. Sci., v. 137, p. 372–374.

Colgrove, G. L., 1940, The Fe-Ni,S system: M.A. thesis, Queen's Univ., Canada.

—— 1942, The system Fe-Ni-S: Ph.D. thesis, Wisconsin Univ., U.S.A..

Craig, J. R., 1967, Violarite stability relations: Carnegie Inst. Washington Year Book 66, p. 434–436.

—— 1971, Violarite stability relations: Am. Mineralogist, v. 56, p. 1303–1311.

—— and Naldrett, A. J., 1971, Phase relations and P_{S_2}-T variations in the Fe-Ni-S system [abs.]: Abstracts of Papers, Geological Association of Canada-Mineralogical Association of Canada Ann. Mtg., Sudbury, Ontario, May 13–15, p. 16–17.

Craig, J. R., Naldrett, A. J., and Kullerud, G., 1967, The 400°C isothermal diagram: Carnegie Inst. Washington Year Book 66. p. 440–441.

Dennen, W. H., 1943, A nickel deposit near Dracut, Mass.: Econ. Geol., v. 38, p. 25–55.

Desborough, G. A., and Carpenter, R. H., 1965, Phase relations of pyrrhotite: Econ. Geol., v. 60, p. 1431–1450.

Desborough, G. A., and Czamanske, G. K., in press, Sulphides in eclogite nodules from a kimberlite pipe, South Africa, with comments on violarite stoichiometry: Am. Mineralogist.

Eckstrand, O. R., 1971, The mineralogy, geochemistry and texture of a low-grade nickeliferous serpentine: Paper presented at Geological Association of Canada-Mineralogical Association of Canada Ann. Mtg., Sudbury, Ontario, May 13–15.

Fleet, M. E., and MacRae, N., 1969, Two-phase hexagonal pyrrhotites: Canadian Mineralogist, v. 9, p, 669–705.

Gehlen, K. von, 1963. Pyrrhotite phase relations at low temperatures: Carnegie Inst. Washington Year Book 62, p. 213–214.

Geller, S., 1962, Refinement of crystal structure of Co_9S_8: Acta Crystallographica, v. 15, p. 1195–1198.

Graterol, M., and Naldrett, A. J., 1971, Mineralogy of the Marbridge No. 3 and No. 4 nickel-iron sulfide deposits: Econ. Geol., v. 66, p. 866–900.

Grønvold, F., and Haraldsen, H., 1952, On the phase relations of synthetic and natural pyrrhotites ($Fe_{1-x}S$): Acta Chemica Scandinavica, v. 6, p. 1452–1469.

Harris, D. C., and Nickel, E. H., 1972, Pentlandite compositions and associations in some mineral deposits: Canadian Mineralogist, v. 11, p. 861–878.

Hillebrand, W. F., 1907, The vanadium sulfide, jatronite, and its mineral associates from Minasraga, Peru: Am. Jour. Sci., ser. 4, v. 24, p. 141–151.

Kalb, G., and Meyer, E., 1926, Die Nickel-und Kobalt führung der Knottenerzlagerstätt von Mechernich: Centralbl. Mineralogie, Abt. A, p. 26.

Karup-Møller, S., 1969, Secondary violarite and bravoite, English Lake, Manitoba: Canadian Mineralogist, v. 9, p. 629–643.

Knop, O., and Ibrahim, M. A., 1961, Chalcogenides of the transition elements. II. Existence of the π-phase in the M_9S_8 section of the Fe-Co-Ni-S: Canadian Jour. Chemistry, v. 39, p. 297–317.

Knop, O., Ibrahim, M. A., and Sutarno, 1965, Chalcogenides of the transition elements. IV. Pentlandite, a natural π phase: Canadian Mineralogist, v. 8, p. 291–316.

Kulagov, T. L., Evstigneeva, T. L., and Yushko-Zakharova, O. E., 1969, The new nickel sulfide, godlevskite: Geol. Rudnykh Mestorozhdeniy, v. 11, p. 115–121.
Kullerud, G., 1956, Subsolidus phase relations in the Fe-Ni-S system: Carnegie Inst. Washington Year Book 55, p. 175–180.
—— 1962, The Fe-Ni-S system: Carnegie Inst. Washington Year Book 61, p. 144–150.
—— 1963a, Thermal stability of pentlandite: Canadian Mineralogist, v. 7, p. 353–366.
—— 1963b, The Fe-Ni-S system: Carnegie Inst. Washington Year Book 62, p. 175–189.
—— Doe, B. R., Buseck, P. R., and Tröften, P. F., 1963, Heating experiments on monoclinic pyrrhotites: Carnegie Inst. Washington Year Book 62, p. 210–213.
Kullerud, G., and Yoder, H. S., 1959, Pyrite stability relations in the Fe-S system: Econ. Geol., v. 54, p. 533–572.
Kullerud, G., and Yund, R. A., 1962, The Ni-S system and related minerals: Jour. Petrology, v. 3, p. 126–175.
Kullerud, G., Yund, R. A., and Moh, G. H., 1969, Phase relations in the Cu-Fe-S, Cu-Ni-S, and Fe-Ni-S systems: Econ. Geol. Mon. 4, p. 323–343.
Lindgren, W., and Davy, W. M., 1924, Nickel ores from Key West mine, Nevada: Econ. Geol., v. 19, p. 309–319.
Lundqvist, D., 1947a, X-ray studies in the ternary system Fe-Ni-S: Arkiv Kemi, Mineralogi, Geologi, v. 24A, no. 22, p. 1–12.
—— 1947b, X-ray studies in the binary system Ni-S: Arkiv Kemi, Mineralogi, Geologi, v. 24A, No. 21, p. 1–12.
Michener, C. E., and Yates, A. B., 1944, Oxidation of primary nickel sulfides: Econ. Geol., v. 39, p. 560–514.
Misra, K. C., 1972, Phase relations in the Fe-Ni-S system: Ph.D. thesis, Univ. of Western Ontario, Canada.
Naldrett, A. J., 1961, The geochemistry of cobalt in the ores of the Sudbury district: M.A. thesis, Queen's Univ., Canada.
—— 1967, Heazlewoodite in the Porcupine district (Ontario): Canadian Mineralogist, v. 8, p. 383–385.
—— Craig, J. R., and Kullerud, G., 1967, The central portion of the Fe-Ni-S system and its bearing on pentlandite exsolution in iron-nickel sulfide ores: Econ. Geol., v. 62, p. 827–847.
Naldrett, A. J., and Gasparrini, E. L., 1971, Archean nickel sulphide deposits in Canada: their classification, geological setting and genesis with some suggestions as to exploration: Geol. Soc. Autralia Spec. Pub. 3.
Naldrett, A. J., Gasparrini, E., Buchan, R., and Muir, J. E., 1972, Godlevskite (β-Ni_7S_6) from the Texmont mine, Ontario: Canadian Mineralogist, v. 11, p. 879–885.
Naldrett, A. J., and Kullerud, G., 1966, Limits of the $Fe_{1-x}S$-$Ni_{1-x}S$ solid solution between 600°C and 250°C: Carnegie Inst. Washington Year Book 65, p. 320–326.
—— 1967, A study of the Strathcona mine and its bearing on the origin of the nickel-copper ores of the Sudbury district, Ontario: Jour. Petrology, v. 8, p. 453–531.
Newhouse, W. H., 1927, The equilibrium diagram of pyrrhotite and pentlandite, and their relations in natural occurrences: Econ. Geol., v. 22, p. 288–299.
Nickel, E. H., 1959, The occurrence of native nickel-iron in the serpentine rock of the Eastern Townships of Quebec province: Canadian Mineralogist, v. 6, p. 307–319.
—— 1972, Nickeliferous smythite from some Canadian occurrences: Canadian Mineralogist, v. 11, p. 514–519.
Owen, E. A., and Liu, Y. H., 1949, Further X-ray study of the equilibrium diagram of the iron-nickel system: Iron and Steel Inst. Jour., v. 163, p. 132–137.
Papunen, H., 1970, Sulfide mineralogy of the Kotalahti and Hitura nickel-copper ores, Finland: Annales Acad. Sci. Fennicae, ser. A, III. Geologica-Geographica, 109, 74 p.
Petruk, W., Harris, D. C., and Stewart, J. M., 1969, Langisite, a new mineral, and the rare minerals cobalt pentlandite, siegenite, parkerite and bravoite from the Langis mine, Cobalt-Gowganda area, Ontario: Canadian Mineralogist, v. 9. p. 597–616.
Popova, G. B., Yershov, V. V., and Kaznetsov, V. A., 1964, Experimental study of the fusion and crystallization of pentlandite: Akad. Nauk SSSR Doklady, v. 156, p. 114–118.
Ramdohr, P., 1950, Über das Vorkommen von Heazlewoodit Ni_3S_2 und über ein neues ihn begleitendes Mineral Shandit Ni_3PbS_2: Deutsche Akad. Wiss., mat.-nat. Kl., Sitzungsber. Jahrg. 1949, no. 6, 31 p.
—— 1967, A widespread mineral association connected with serpentinization: Neues Jahrb. Mineralogie, Abh., v. 117, p. 241–265.
Rucklidge, J., 1967, Electron micro-probe analytical data reduction programme: Unpub. rept., Dept. of Geology, Univ. of Toronto, Canada.
Sandefur, B. T., 1942, The geology and paragenesis of the nickel ores of the Cuniptau mine, Goward, Nipissing district, Ontario: Econ. Geol., v. 37, p. 173–187.
Shewman, R. W., 1966, Pentlandite phase relations in the Fe-Ni-S system and the stability of the pyrite-pentlandite assemblages: M.Sc. thesis, McGill Univ., Canada.
—— and Clark, L. A., 1970, Pentlandite phase relations in the Fe-Ni-S system and notes on the monosulfide solid solution: Canadian Jour. Earth Sci., v. 7, p. 67–85.
Shimazaki, H., 1971, Thermochemical stability of bravoite: Econ. Geol., v. 66, p. 1080–1082.
Short, M. N., and Shannon, E. V., 1930, Violarite and other rare nickel sulfides: Am. Mineralogist, v. 15, p. 1–17.
Springer, G., Schachner-Korn, D., and Long, J. V. P., 1964, Metastable solid solution relations in the system FeS_2-CoS_2-NiS_2: Econ. Geol., v. 59, p. 475–491.
Stumpfl, E. F., and Clark, A. M., 1964, A natural occurrence of Co_9S_8, identified by X-ray microanalysis: Neues Jahrb. Mineralogie, Abh., v. 101, p. 240–245.
Taylor, L. A., 1969, Low-temperature phase relations in the Fe-S system: Carnegie Inst. Washington Year Book 68, p. 259–270.
Thomson, J. E., and Allen, J. S., 1939, Nickeliferous pyrite from the Denison mine, Sudbury district, Ontario: Univ. Toronto Studies, Geol. Ser., v. 42, p. 135–138.
Ulrich, G. H. F., 1890, On the discovery, mode of occurrence and distribution of nickel-iron alloy awaruite on the west coast of South Island, New Zealand: Geol. Soc. London Quart. Jour., v. 46, p. 619–633.
Urazov, G. G., and Filin, N. A., 1938, Investigation of the ternary iron-nickel-sulfur system [in Russian]: Metallurgie, v. 13, p. 3–17.
Vaughan, D. J., 1969, Zonal variation in bravoite: Am. Mineralogist, v. 54, p. 1075–1083.
—— Schwarz, E. J., and Owens, D., 1971, Pyrrhotite from Strathcona mine, Sudbury, Canada; a thermal magnetic mineralogical study: Econ. Geol., v. 66, p. 1131–1144.
Vogel, R., and Tonn, W., 1930, The ternary system Fe-Ni-S: Archiv Eisenhuttenwessen, v. 12, p. 769.
Walker, T. L., 1894, Notes on nickeliferous pyrite from Murray mine, Sudbury, Ont.: Am. Jour. Sci., ser. 3, v. 47, p. 312–314.
—— 1915, Certain mineral occurrences in the Worthington mine, Sudbury, Ontario and their significance: Econ. Geol., v. 10, p. 536–543.
Wandke, A., and Hoffman, R., 1924, A study of the Sudbury ore deposits: Econ. Geol., v. 19, p. 169–204.
Watkinson, D. H., and Irvine, T. N., 1964, Peridotitic intrusions near Quetico and Shebandowan, northwestern Ontario: A contribution to the petrology and geochemistry of ultramafic rocks: Canadian Jour. Earth Sci., v. 1, p. 63–98.
Williams, K. L., 1958, Nickel mineralization in Western Tasmania: Australian Inst. Mining Metallurgy, Stillwell Anniversary Vol., p. 263–302.
—— 1960, An association of awaruite with heazlewoodite: Am. Mineralogist, v. 45. p. 450–453.
Yund, R. A., and Hall, H. T., 1968, The miscibility gap between FeS and $Fe_{1-x}S$: Materials Research Bull., v. 3, p. 779–784.
—— 1969, Hexagonal and monoclinic pyrrhotites: Econ. Geol., v. 64, p. 420–423.
Zurbrigg, H. F., 1933, A study of nickeliferous pyrrhotites: M. A. thesis, Queen's Univ., Canada.